DOKUZ EYLÜL UNIVERSITY
GRADUATE SCHOOL OF NATURAL AND APPLIED
SCIENCES

BOLT-HOLE TIGHTENING EFFECTS IN SINGLE-LAP COMPOSITE BOLTED JOINTS

by
Esmaeil GHANBARI

June, 2011
İZMİR

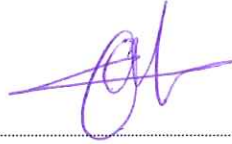# BOLT-HOLE TIGHTENING EFFECTS IN SINGLE-LAP COMPOSITE BOLTED JOINTS

A Thesis Submitted to the

Graduate School and Applied Sciences of Dokuz Eylül University

In Partial Fulfillment of the Requirements for the

Degree of Master of Science in

Mechanical Engineering, Mechanics Program

by
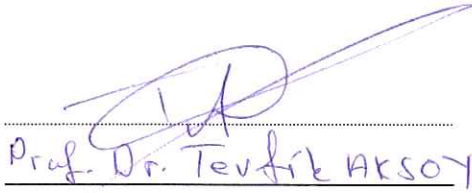**Esmaeil GHANBARI**

June, 2011
İZMİR

M.Sc THESIS EXAMINATION RESULT FORM

We have read the thesis entitled **"BOLT-HOLE TIGHTENING EFFECTS IN SINGLE-LAP COMPOSITE BOLTED JOINTS"** completed by **ESMAEIL GHANBARI** under supervision of **PROF. DR. ONUR SAYMAN** and we certify that in our opinion it is fully adequate, in scope and in quality, as a thesis for the degree of Master of Science.
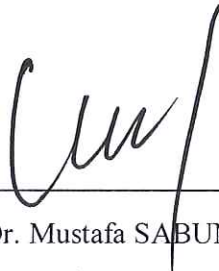
Prof. Dr. Onur SAYMAN

Supervisor

Prof. Dr. Tevfik AKSOY

(Jury Member)

Prof. Dr. Ramazan KARAKUZU

(Jury Member)

Prof.Dr. Mustafa SABUNCU

Director

Graduate School of Natural and Applied Sciences

ACKNOWLEDGEMENTS

BOLT-HOLE TIGHTENING EFFECTS IN SINGLE-LAP COMPOSITE BOLTED JOINTS

ABSTRACT

The weight and fuel savings offered by composite materials make them attractive not only to the military, but also to the civilian aircraft, aerospace, and automotive industries, where bolting joints are extensively used as a primary method of forming structural joints. Single-lap joints have good accordance with real conditions in comparison with other joint types. Therefore, the main objective of this paper is to investigate the behavior of single-lap joints in glass fiber reinforced epoxy (GFRE) composites under tension and pure bending loading conditions, with a constant W/D ratio (3) and variable the E/D ratios (3, 4, 5) and tightening torque values (0, 3 and 6 Nm). First, the mechanical properties of the composite were determined experimentally using the ASTM testing standards. Bending properties were determined using four-point bending test. During the tests, the tabs were bonded to the ends of plates to eliminate the secondary bending effects during tension test and to obtain symmetric geometry at bending test. Finally, special test fixtures were designed to facilitate the study of the effect of bending on the composite bolted joints.

The experimental results show that in the tension tests, with increasing E/D ratio and tightening torque, the value of failure bearing stress increased. But, it seems that, this is not always true for continuous increase of these parameters. And in the bending tests, it is seen that at zero torque, with the increase of the E/D ratio the bending strength value increases, but this increase is small at T=3, 6 Nm torques. And in these tests, the joint failed at the center, near the bolt, because of the excessive delaminations on the compressive side.

Key words: Failure load, Single-lap joint, Composite laminate, Four point bending, Bolting joint

TEKİL YAPIŞTIRILMIŞ KOMPOZİT CİVATALANMIŞ BAĞLANTILARDA CİVATA DELİK SIKI GEÇME ETKİLERİ

ÖZ

Kompozit malzemeler tarafından sunulan ağırlık ve yakıt tasarufu sadece askeri uygulamalarda değil ayrıca sivil havacılık, uzay uygulamaları ve otomotiv endüstrisinde de onları çekici kılmaktadır ki bu uygulamalarda civatalı bağlantılar, yapısal bağlantıların şekillendirilmesinin ilk yöntemi olarak yoğun şekilde kullanılmaktadır. Tekil bindirmeli bağlantılar, gerçek uygulamalarda diğer tip bağlantılarla kıyaslandığında iyi bir uyuma sahiptirler. Bu yüzden bu çalışmanın temel konusu, sabit W/D oranına (3) ve değişken E/D oranlarına (3, 4, 5) ve sıkıştırma tork değerlerine (0, 3, 6 Nm) sahip cam elyaf takviyeli kompozitlerin çekme ve salt eğilme yüklemesi durumlarındaki davranışlarını incelemektir. İlk olarak kompozitin mekanik özellikleri ASTM test standartları kullanılarak deneysel olarak belirlenmiştir. Eğilme özellikleri dört nokta eğilme testi kullanılarak belirlenmiştir. İnce plakalar, çekme testleri esnasında ikincil eğilme etkilerini ortadan kaldırabilmek ve eğilme testleri esnasında da geometriye simetriklik kazandırabilmek amacı ile uç kısımlarından birbirlerine yapıştırılmıştır. Son olarak ise özel test aparatı, civatalı kompozit bağlantıların eğilmesinin etkilerini kolaylaştırmak amacı ile tasarlanmıştır.

Deneysel sonuçlar, artan E/D oranı ve sıkıştırma tork değerlerinin çekme testinde, hasar yatak gerilmesinin değerinin artığını göstermektedir. Fakat, bu yorum parametrelerin sürekli olarak artması durumunda daima doğru değildir. Ve eğilme testlerinde, tork uygulanmadığı zaman, E/D oranının artması eğilme mukavemetini artırmaktadır, fakat bu artış T=3, 6 Nm'de küçüktür. Bu testlerde, bağlantı sıkıştırma alanı üzerindeki aşırı delaminasyondan dolayı merkezde ve civatanın yanında hasara uğramıştır.

Anahtar Kelimeler: Hasar yükü, Tekil bindirmeli bağlantı, Kompozit tabaka, Dört nokta eğme, Civatalı Bağlantıar

CONTENTS   Page

CHAPTER ONE

INTRODUCTION

1.1 Overview

The use of composite materials in structural components of mechanical and civil applications has grown steadily in recent years. Today, many composite parts are made out of unidirectional prepreg tapes and are being used extensively in applications where a joint is required. In composite structures, three types of joints are commonly used, namely, mechanically fastened joints, adhesively bonded joints, and hybrid mechanically fastened/adhesively bonded joints. Bolted joints or hybrid bolted/bonded joints are still the dominant fastening mechanisms used in joining of primary structural parts made from advanced composites. Mechanical fasteners offer the advantage of being able to be removed without destroying the structure and they are not sensitive to surface reparation, service temperature, or humidity. The procedure for designing mechanically fastened joints in composite materials is predominately based on experimental data and the analytical models are largely empirical in nature. The selection of appropriate or optimum geometric parameters and materials are essential in order to achieve the structural integrity and reliability in composite structures, since bolted joints in composites fail at loads that are not predicted by either perfectly elastic or perfectly plastic assumptions. Any joint in a composite structure, if not designed appropriately, may act as a damage initiation point and may lead to failure of the component at that location.

A major goal of bolted joint research is to determine the effect of various bolting parameters on the bearing strength of the joint .These parameters include: (a) joint geometry (specimen width, end distance, and hole diameter); (b) joint configuration (single over lap, double lap, single bolt, single bolt row, or multi-bolt row); (c) loading condition (tension, compression or combined static and/or fatigue loading); (d) fastening parameters (bolt/hole clearance, bolt/washer clearance, tightening torque or clamping force, washer size, and presence of countersink); and (e) material parameters (stacking sequence, fiber shape, matrix type, fiber volume fraction). In summary, the joints would be expected to eventually fail in a variety of modes; namely, net-tension, shearing-out,

and bearing Figure 1.1. In terms of structural design, bearing failure preferably occurs as a combination of these three modes, in view of stability of the failure process. However, bearing failure is a local compressive failure mode due to contact and frictional forces acting on the surface of the hole. This fracture process is very complicated and is influenced by many parameters, including edge to hole distance and lateral clamping force.
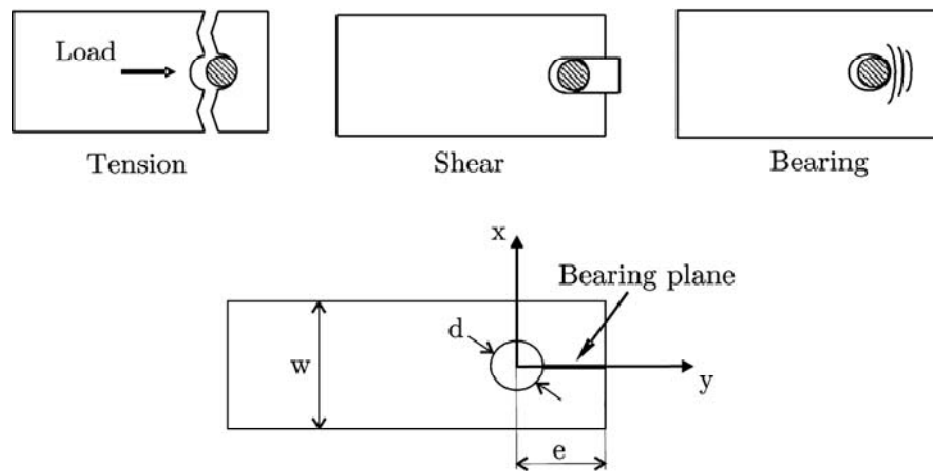
Figure 1.1 Failure modes of composites structural

Though a large body of literature exists on composite bolted joints, McCarthy et al.(2002) examined single lap, single-bolt specimens made from high-strength graphite/epoxy laminates with quasi-isotropic and zero-dominated lay-ups. The bolts were 8 mm in diameter and clearances examined were neat-fit, 80, 160 and 240μm. They followed the procedures in ASTM standard D5961/D5961 M-96 (1996), and similarly to DiNicola AJ, Fantle SL (1993) found no effect of clearance on ultimate tensile strength of the joints, but for 2% offset strength (which in single lap joints corresponds to 4% HDS) they found a 7–8% loss of strength from neat-fit to the largest clearance. They also suggested an alternative measure of strength based on the bearing stress at a given percentage loss in stiffness of the joint. The strength values from this criterion are generally below those for the 2% offset criterion, and may be more closely correlated with the occurrence of first significant damage, such as occurs in bearing failure. They found that clearance had a stronger effect on this strength measure (up to 14% loss from neat-fit to the largest clearance) than on the 2% offset strength.

Crews (1981) conducted static and fatigue tests under bolt-bearing loads for a range of bolt clamp-up torques. He reported that bolt clamp-up force exerts a significant effect on both static strength and fatigue limit.

Wang et al. (1996) used bearing response and bearing strength of bolted joints to examine the bearing failure mechanism as a function of clamping pressure. In their work, a pin-loaded bearing (without lateral clamping) test and a bolted bearing (with lateral clamping) test were conducted to evaluate the bearing damage.

Aktas and Karakuzu (1999) worked on pin connections of continuous fiber reinforced epoxy composite laminates, investigated the loading, which causes damage on the connections, and the failure types experimentally and numerically.

Chang and Scott (1982) investigated the laminates, which are fibers reinforced having different layers and different configurations.

Collings (1977) investigated the variables such as, layer orientation, laminate thickness, and bolt compression pressure. Collings (1982) also worked on the relationship between connection strength and joint parameters.

Kashaba (1996) investigated the effect of fiber volume ratio to the bearing strength of the material.

Okutan et al. (2001) experimentally investigated the load carrying properties of Kevlar/epoxy composite laminates. It is well known that depending on the joint geometry, a pin-loaded composite can exhibit different failure modes.

Concerning multi-bolt joints, Fan and Qiu (1993) performed a two-dimensional analytical study of the effects of clearance on load distribution in multi-bolt joints. They studied a four-fastener, single-shear joint and clearances examined included neat-fit, 30lm and 60lm, in 5mm diameter holes. They found that with clearance fits in the inner two holes, a substantial amount of the load was transferred to the outer two bolts. They also found that the load distribution in this case became more even as the load increased.

However, no experimental verification was performed. McCarthy and McCarthy (2003) performed a three-dimensional finite element study of three-bolt, single-lap joints involving 8mm bolts and clearances ranging from neat-fit to 160lm. They found that a loose-fitting outer bolt resulted in the two neat-fit bolts taking virtually all the load up to quite high loads (with all bolts initially centered in the holes). Their analysis however did not consider non-linear material behavior or joint failure. Experimental studies of the effects of bolt–hole clearance on strength and fatigue life of multi-bolt joints have not so far appeared in the open literature.

Kim (1987) stated that when a loose bolt in a hole is shifted back and forth, the hole elongates at an increasing rate and failure occurs. He also stated that it is important that all bolts in composites fit neatly. However neither of these publications gave a clear definition of just how much clearance is acceptable or how much the strength and fatigue life is reduced by loose bolts. Therefore some quantified information on this subject is desirable.

Eriksson (1990) has shown that bearing strength is influenced by several important parameters, including lateral constraint conditions and ply orientations.

Wu and Sun (1998) investigated the behavior of pin-contact failure of composite laminates and found that fiber micro-buckling in the 0-deg plies of the laminate plays an important role in the initiation of bearing damage.

Camanho et al. (1998) carried out a detailed experimental investigation for three basic failure modes of a joint, and their results show that the main mechanism of bearing failure is accumulated delamination damage.

The effect of clearance on joint stiffness was not reported. Pierron et al. (2000) investigated clearances in ±45° woven glass fiber epoxy pin joints, both experimentally and with finite element analysis. Clearances of 0.1, 0.5, 1, 1.5 and 2 mm with pins of 16 mm diameter were examined. The load deflection curves for their configurations had a smooth non-linear shape until a clear load drop-off at failure. The failure load was found to decrease by 30% from 0.1 mm clearance to 2 mm clearance. They also concluded that the joint stiffness did not vary much but did not quantify this. However,

approximate measurements from their load deflection curves would seem to indicate a drop in stiffness of 15–20%, which is quite substantial.

Naik and Crews (1986) made the similar conclusion from their finite element study that clearance should be considered in strength analyses, but may have little effect on joint stiffness.

Ireman (1995) performed experimental and three-dimensional finite element studies on single-bolt, single-lap joints (without considering variable clearance) and demonstrated the three-dimensional nature of the stresses and failure propagation in such cases. The single-lap, single bolt joint is one of the standard configurations for characterisation of mechanically fastened composite joints in MIL-HDBK-17 and in ''ASTM Standard D 5961/D 5961M- 96, Standard test Method for Bearing Response of Polymer Matrix Composite Laminates'' (1996). MIL-HDBK-17 states that the single-lap configuration is more representative than the double-lap configuration of most critical aircraft bolted joint applications. Single-lap joints result in significant stress concentrations in the thickness direction and lower bearing strengths (1995).

Whitworth et al. (2003) carried out an analysis to assess the bearing strength of pin-loaded composite joints. The analysis involved by using the Chang–Scott–Springer characteristic curve model and a two-dimensional finite element analysis to obtain the stress distribution around the fastener hole.

Aktas and Dirikolu (2003) investigated a pin loaded carbon epoxy composite laminate with different stacking sequences in order to determine its safe and maximum bearing strengths, experimentally.

Tong (2000) reported an experimental investigation on the effect of non-uniform bolt-to-washer radial clearance on bearing failure of bolted joints under different clamping forces with various lateral constraints. The experimental results were also used to validate an existing model. Two extreme diametral fit positions, with a positive or negative bolt hole-to-washer clearance, were also considered.

Hamada and Maekawa (1996) studied failure analysis of quasi-isotropic carbon epoxy laminates both numerically and experimentally. Meola et al. (2003) studied an

experimental investigation on an innovative glare fiber reinforced metal laminate (FRML) with the aim to characterize its strength and behavior in the case of mechanical joints. Several specimens were fabricated by varying width and hole-to-edge distance and tested in pin-bearing way without lateral restraints, which was the most critical testing procedure in the simulation of mechanical joints. Specimens, after bearing stress, were analyzed in both nondestructive and destructive ways. Meanwhile, a method was presented for predicting the failure strength and failure mode of mechanically fastened fiber reinforced composite laminates by Chang et al. (1982).

In the present study, the effects of tightening torque and edge distance-to-hole diameter (E/D) on the strength of bolted joint in single-lap joints with tabs that are bonded to the ends of the test specimens and fabricated from glass fiber reinforced epoxy composite materials, are investigated experimentally. The composites have a stacking sequence of $[0/45/30/-30/-30/30/45/0]_s$ and are subjected to the traction and four point bending moment tests. The mechanical properties of the composite laminate (tension, compression, and shear) are determined experimentally.

CHAPTER TWO

INTRODUCTION TO COMPOSITE MATERIALS

2.1 Characteristics of a Composite Material

The constituents of a composite are generally arranged so that one or more discontinuous phases are embedded in a continuous phase. The discontinuous phase is the reinforcement and the continuous phase is the matrix (Staab G. H. 1992). An exception to this is rubber particles suspended in a rigid rubber matrix, which produces a class of materials known as rubber-modified polymers. In general the reinforcements are much stronger and stiffer than the matrix. Both constituents are required, and each must accomplish specific tasks if the composite is to perform as intended.

A material is generally stronger and stiffer in fiber form than in bulk form. The numbers of microscopic flaws that act as fracture initiation sites in bulk materials are reduced when the material is drawn into a thinner section. In fiber form the material will typically contain very few microscopic flaws from which cracks may initiate to produce catastrophic failure. Therefore, the strength of the fiber is greater than the bulk material. Without a binder material to separate them, they can become knotted, twisted, and hard to separate. The binder (matrix) material must be continuous and surround each fiber so that they are kept distinctly separate from adjacent fibers and the entire material system is easier to handle and work with.

The physical and mechanical properties of composites are depend on the properties, geometry, and concentration of the constituents. Increasing the volume content of reinforcements can increase the strength and stiffness of a composite to a point. If the volume content of reinforcements is too high there will not be enough matrix to keep them separate, and they can become tangled. Similarly, the geometry of individual reinforcements and their arrangement within the matrix can affect designing with composite materials. The type of reinforcement and matrix, the geometric arrangement and volume fraction of each constituent, the anticipated mechanical loads, the operating environment for the composite and so forth must all be taken into account.

Analysis of composites subjected to various mechanical, thermal, and hygral conditions is the main thrust of this text. Discussions are limited to continuous fiber laminated composites. In introductory strength of materials, the constitutive relationship between stress and strain was established for homogeneous isotropic materials as Hooke's law. A composite material is analyzed in a similar manner, by establishing a constitutive relationship between stress and strain.

Isotropic, homogeneous materials (steel, aluminum, etc.) are assumed to be uniform throughout and to have the same elastic properties in all directions. Upon application of a uniaxial tensile load, an isotropic material deforms in a manner similar to that indicated in Figure2.1. In this figure undeformed specimen showed with dashed lines. Assuming a unit width and thickness for the specimen, the transverse in-plane and out-of-plane displacements are the same. Unlike conventional engineering materials, a composite material is generally nonhomogeneous and does not behave as an isotropic material. Most composites behave as either anisotropic or orthotropic materials.
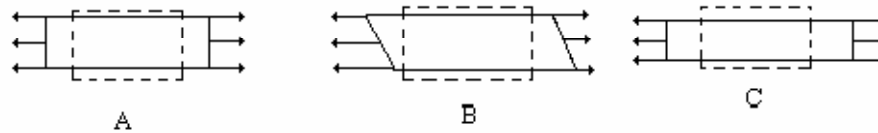
Figure 2.1 Isotropic (A), anisotropic (B), and orthotropic (C) materials responses subjected to axial tension.

The material properties of an anisotropic material are different in all directions. There is typically a coupling of extension and shear deformation under conditions of uniaxial tension. The response of an anisotropic material subjected to uniaxial tension is also shown in Figure 2.1. There are varying degrees of anisotropic material.

Behavior and the actual deformation resulting from applied loads depends on the material. The material properties of an orthotropic material are different in three mutually perpendicular planes, but there is generally no shear-extension coupling as with an anisotropic material. The transverse in-plane and out-of-plane displacements are not typically the same, because Poisson's ratio is different in these two directions. Figure 2.1 shows orthotropic material response too. Although it appears similar to that of

an isotropic material, the magnitudes of the in-plane and out-of-plane displacements are different.

2.2 Classification of Composite Materials

It's known that composites have two (or more) chemically distinct phases on a microscopic scale, separated by a distinct interface, and it is important to be able to specify these constituents. The constituent that is continuous and is often, but not always, present in the greater quantity in the composite is termed the matrix. The normal view is that it is the properties of the matrix. That is improved upon when incorporating another constituent to produce a composite. A composite may have a ceramic, metallic or polymeric matrix. The mechanical properties of these classes of material differ considerably. As a generalization, polymers have low strengths and Young's moduli, ceramics are strong, stiff and brittle, and metals have intermediate strengths and moduli, together with good ductilities, i.e. they are not brittle.

The second constituent is known to as the reinforcing phase, or reinforcement, as it enhances or reinforces the mechanical properties of the matrix. In most cases the reinforcement is harder, stronger and stiffer than the matrix, although there are some exceptions; for example, ductile metal reinforcement in a ceramic matrix and rubberlike reinforcement in a brittle polymer matrix. At least one of the dimensions of the reinforcement is small, say less than 500 μm and sometimes only of the order of a micrometer. The geometry of the reinforcing phase is one of the major parameters in determining the effectiveness of the reinforcement; in other words, the mechanical properties of composites are a function of the shape and dimensions of the reinforcement. We usually describe the reinforcement as being either fibrous or particulate. Figure 2.2 represents a commonly employed classification scheme for composite materials which utilizes this designation for the reinforcement (Figure 2.2 – Block A)
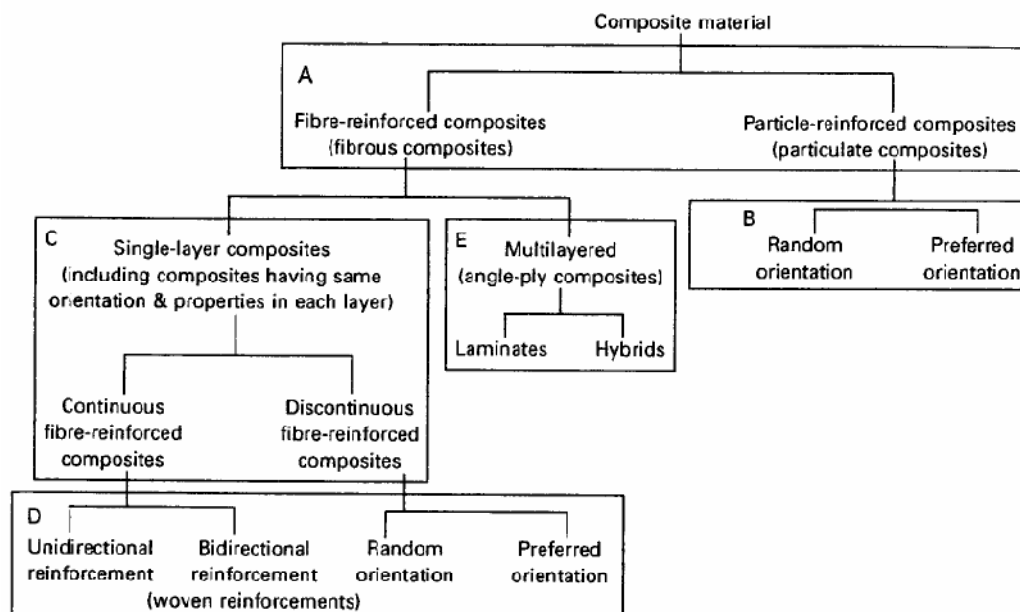
Figure 2.2 Classifications of composite materials

Particulate reinforcements have dimensions that are approximately equal in all directions the shape of the reinforcing particles may be spherical, cubic, platelet or any regular or irregular geometry. The arrangement of the particulate reinforcement may be random or with a preferred orientation, and this characteristic is also used as a part of the classification scheme (Figure 2.2 Block B). In the majority of particulaterein forced composites the orientation of the particles is considered, for practical purposes, to be random.

A fibrous reinforcement is characterized y its length being much greater than its cross-section dimensions. However, the ratio of length to a cross-section dimension, known as the aspect ratio, can vary considerably. In single-layer composites long fibers with high aspect ratios give what are called continuous fiber-reinforced composites, whereas discontinuous fiber composites are fabricated using short fibers of low aspect ratio (Figure 2.2 Block C). The orientation of the discontinuous fibers may be random or preferred. The frequently encountered preferred orientation in the case of a continuous fiber composite is termed unidirectional and the corresponding random situation can be approximated to by bidirectional woven reinforcement (Figure 2.2 Block D).

Multilayered composites are another category, and commonly used form, of fiber reinforced composites. These are classified as either laminates or hybrids (Figure 2.3 Block E). Laminates are sheet constructions which are made by stacking layers (also called plies or laminate and usually unidirectional) in a specified sequence. The layers are often in the form of 'prepreg' (fibers pre-impregnated with partly cured resin) which are consolidated in an autoclave. A laminate may have between 4 and 400 layers and the fibre orientation changes from layer to layer in a regular manner through the thickness of the laminate, e.g. a (0/90/0) stacking sequence results in a cross-ply composite.

Hybrids are composites with mixes fibers and are becoming commonplace. The fibers may be mixed within a ply or layer by layer, and these composites are designed to benefit from the different properties of the fibers employed. For example, a mixture of glass and carbon fibers incorporated into a polymer matrix gives a relatively inexpensive composite, owing to the low cost of glass fibers, but with mechanical properties enhanced by the excellent stiffness of carbon.

2.3 Composite Material Terminology

2.3.1 Lamina

A lamina is a flat or a curved collection of unidirectional or woven fibers suspended in a matrix material. A lamina is usually assumed to be orthotropic, and the material from which it is made designate its thickness. For example, a graphite/epoxy lamina may be on the order of 0,127mm thick. For the purpose of analysis, a lamina is naturally modeled as having one layer of fibers through the thickness. This is only a model and not a true representation of fiber arrangement. Unidirectional and woven laminas are schematically illustrated in Figure 2.3.
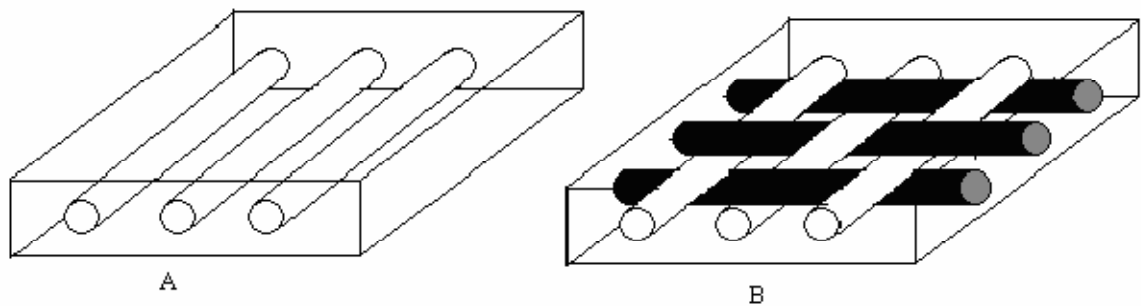
Figure 2.3 Schematic illustration of A: unidirectional; B: oven composites

2.3.2 Reinforcement Material

Reinforcements are used to create the composite structure stronger. The most usually used reinforcements are boron, glass, graphite, kevlar, aluminum, silicon carbide, silicon nitride and titanium

2.3.3 Fiber Material

Fibers are a special case of reinforcements. They are generally continuous and have diameters ranging from 3 to 200μm. Fibers are typically linear elastic or elastic perfectly plastic and are generally stronger and stiffer than the same material in bulk form. The most commonly used fibers are boron, glass, carbon and kevlar.

2.3.4 Matrix Material

The matrix is the binder material that supports, separates, and protects the fibers. It provides path by which load is both transferred to the fibers and redistributed among the fibers in the event of fiber breakage. The matrix typically has a lower density, stiffness, and strength than the fibers. Matrices can be brittle, ductile, elastic, or plastic. They can have either linear or nonlinear stress-strain behavior. In addition, the matrix material must be capable of being forced around the reinforcement during some stage in the manufacture of the composite. Fibers must often be chemically treated to ensure proper adhesion to the matrix. The most commonly used matrices are carbon, ceramic, metal, and polymeric. Each has special appeal and usefulness, as well as limitations and given below (Richardson, 1987).

1. Carbon matrix: A carbon matrix has a high heat capacity per unit weight. They have been used as rocket nozzles, ablative shields for reentry vehicles, and clutch and brake pads for aircraft.

2. Ceramic matrix: A ceramic matrix is frequently brittle. Carbon, ceramic, metal, and glass fibers are typically used with ceramic matrices in areas where extreme environments are anticipated.

3. Glass matrix: Glass and glass-ceramic composites frequently have an elastic modulus much lower than that of the reinforcement. Carbon and metal oxide fibers are the most general reinforcements with glass matrix composites. The best characteristics of glass or ceramic matrix composites are their strength at high service temperatures. The primary applications of glass matrix composites are for heat-resistant parts in engines, exhaust systems, and electrical components.

4. Metal matrix: A metal is especially good for high-temperature use in oxidizing environments. The most commonly used metals are iron, nickel, tungsten, titanium, magnesium, and aluminum. There are three classes of metal matrix composites.

   a) Class 1: The reinforcement and matrix are insoluble. Reinforcement/matrix combinations in this class include tungsten or alumina/copper, BN-coated B or boron/aluminum, and boron/magnesium.

   b) Class 2. The reinforcement/matrix exhibits some solubility and the interaction will alter the physical properties of the composite. Reinforcement/matrix combinations included in this class are carbon or tungsten/nickel, tungsten/columbium, and tungsten/copper.

   c) Class 3. The most critical situations in terms of matrix and reinforcement are in this class. The problems encountered here are generally of a manufacturing nature and can be solved through processing controls. Within these classes the reinforcement/matrix combinations include alumina or boron or silicon carbide/titanium, carbon or slica/aluminum, and tungsten/copper.

5. Polymer matrix: Polymeric matrices are the most common and least expensive. They are found in nature as amber, pitch, and resin. Some of the earliest composites were layers of fiber, cloth, and pitch. Polymers are easy to process,

offer good adhesion. They are a low-density material. Because low processing temperatures, many organic reinforcements can be used. A typical polymeric matrix is either viscoelastic or viscoplastic, meaning it is affected by time, temperature, and moisture. The terms thermoset and thermoplastic are often used to identify a special property of many polymeric matrices as,

a) Thermoset: A thermoset matrix has greatly cross-linked polymer chains. After it has been processed a thermoset can not be remolded. Thermoset matrices are sometimes used at higher temperatures for composite applications.

b) Thermoplastic: A thermoplastic matrix has polymer chains that are not cross-linked. Although the chains can be in contact, they are not linked to each other. A thermoplastic can be remolded to a new shape when it is heated to approximately the same temperature at which it was formed.

2.3.5 Laminate

A laminate is prepared two or more unidirectional laminate or plies stacked together at various orientations Figure 2.4. The laminate can be a range of thickness and consist of different materials (Daniel, and Ishai, 1994).

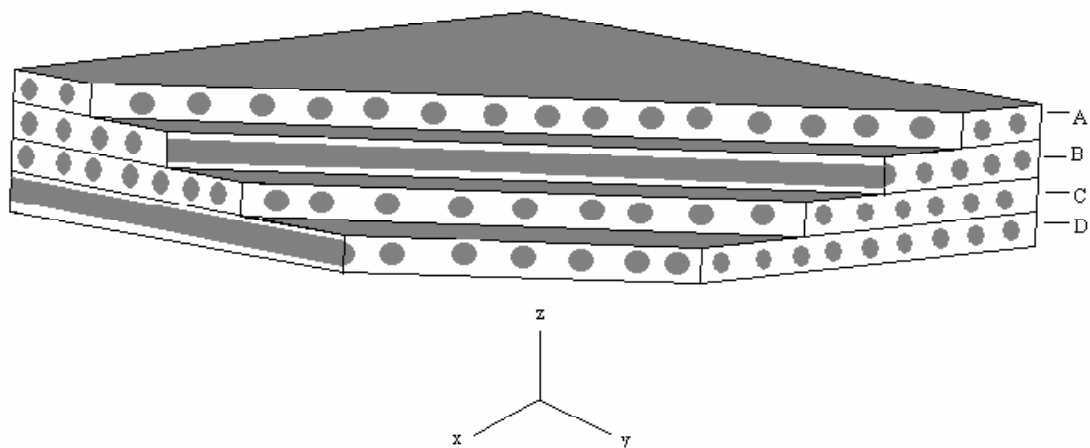Figure 2.4 Multidirectional laminate with reference coordinate system; A = 00, B =-θ0, C = + θ0 D = 900

As the principal material axes differ from ply to ply, it is more convenient to analyze laminates using a common fixed system of coordinates. The orientation of a given ply is

given by the angle between the references x- axis and the major principal material axis (fiber orientation) of the ply, measured in a counterclockwise direction x-y plane.

Composite laminates containing plies of two or more different types of materials are named hybrid composites and more specifically interply hybrid composites. For instance, a composite laminate may be made up of unidirectional glass/epoxy, carbon/epoxy and aramid/epoxy layers stacked together in a specified sequence. In some cases it may be advantageous to intermingle different types of fibers, such as glass and carbon or aramid and carbon, within the same unidirectional ply. These composites are intraply hybrid composites. One could combine intraply hybrid layer with other layers to form an intraply-interply hybrid composite.

Composite laminates are created in a manner indicating the number, type, orientation and stacking sequence of the plies. Lay-up is the design of the laminate indicating its ply composite. The design indicating, in addition to the ply composition, the exact location or sequence of the various plies is named the stacking sequence. Composite designations are given below in Table 2.1.

Table 2.1 Laminate designations

S= Symmetric sequence, T= Total number of plies, = Laminate is symmetric about the midplane of the ply, Number subscript= Multiple of plies, K= Kevlar, C= Carbon,   G= Glass fibers

Unidirectional	6-ply [0/0/0/0/0/0] = $[0_6]$
Crossply	[0/90/90/0] = $[0/90]_s$ [0/90/0] = $[0/90]_s$
Angle-ply symmetric	[+45/-45/-45/+45] = $[\pm45]_s$ [30/-30/30/-30/-30/30/-30/30] = $[\pm30]_{2s}$
Angle-ply asymmetric	[30/-30/30/-30/30/-30/30/-30] = $[\pm30]_{4s}$
Multi directional	[0/45/-45/-45/45/0] = $[0/\pm45]_s$ [0/0/45/-45/0/0/0/0/-45/45/0/0] = $[0_2/\pm45/0_2]_s$ [0/15/-15/15/-15/0] =$[0/\pm15/\pm15/0]_T = [0/(\pm15)2/0]_T$
Hybrid	$[0_K/0_K/45_C/-45_C/90_G/-45_C/45_C/0_K/0_K]_T = 0_{K2}/\pm45_C/90_G]_s$

2.4. **Micromechanics and Macro Mechanics**

Composite materials can be viewed and analyzed at different levels and on different scales, depending on the particular characteristic and behavior under consideration. A schematic diagram of the various steps of consideration and the corresponding types of analysis is given in Figure 2.5.
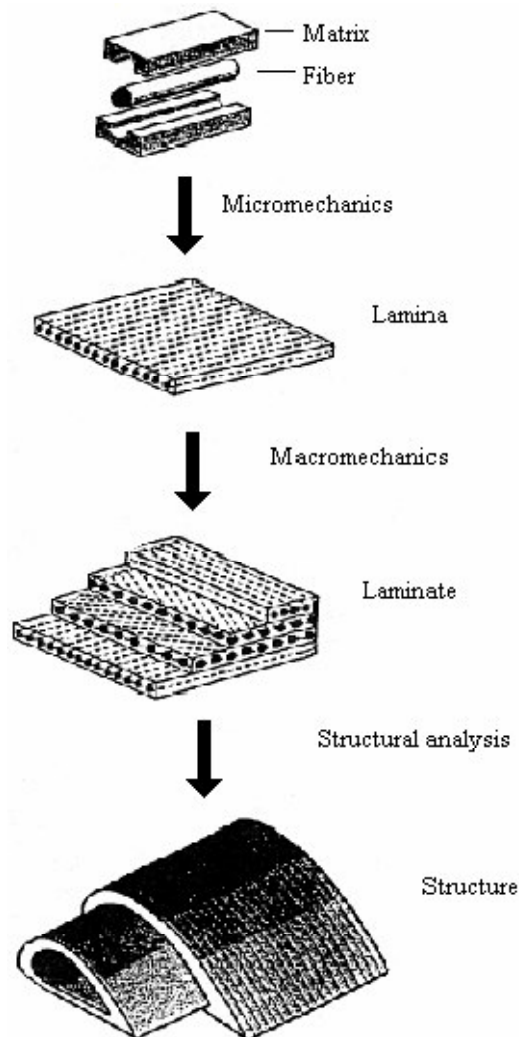

Figure 2.5 Steps of observation and types of analysis for composite materials

At the constituent step the scale of examination is on the border of the fiber diameter, particle size or matrix interstices between reinforcement. Micromechanics are the study of the interactions of the constituents on this microscopic level. It deals with the state of

deformation and stress in the constituents and local failures such as matrix failure (tensile, compressive, shear), fiber failure (tensile, buckling, splitting) and interface/interphase failure. An example of the complex stress distributions on the transverse cross section of a transversely loaded unidirectional composite is given in Figure 2.6.
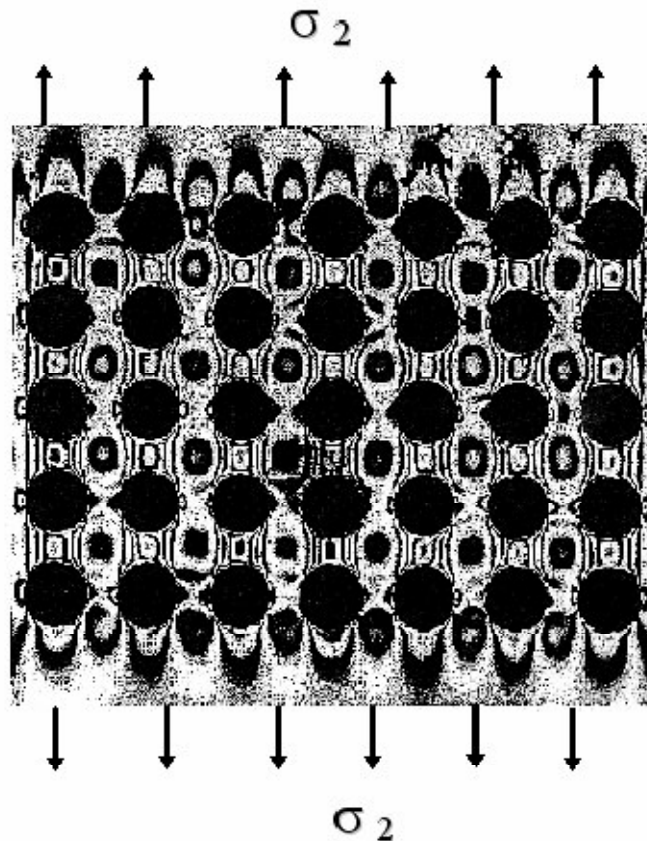
Figure 2.6 Isochromatic fringle patterns in a model of transversely
loaded unidirectional composite

Micromechanics is particularly important in the study of properties such as strength, fracture toughness, and fatigue life, which are powerfully influenced by local characteristics that can not be integrated or averaged. Micromechanics also allow the prediction of average behavior at the lamina level as a function of constituent properties and local conditions.

At the lamina step it usually more expeditious to consider the material homogeneous, albeit anisotropic and use average properties in the analysis. This type of analysis is called macromechanics and considers the unidirectional lamina as a quasi homogeneous anisotropic material with its own average stiffness and strength properties. Failure criteria may be expressed in terms of average stresses and overall lamina strengths without reference to any particular local failure mechanisms. This approach is recommended in the study of the overall elastic or viscoelastic behavior of composite laminates or structures which assumes material continuity.

At the laminate step the macromechanical analysis is performed in the form of lamination theory dealing with overall behavior as a function of lamina properties and stacking sequence. At the component or structure level, methods such as finite element analysis coupled with lamination theory give the overall behavior of the structure as well as the state of stress in each lamina.

2.5 Special Features of Composites

Composites have been routinely designed and manufactured for applications in which high performance and light weight are needed. They offer several advantages over traditional engineering materials as discussed below.

- Composite materials provide capabilities for part integration. Several metallic components can be replaced by a single composite component.
- Composite structures provide in-service monitoring or online process monitoring with the help of embedded sensors. This feature is used to monitor fatigue damage in aircraft structures or can be utilized to monitor the resin flow in an RTM (resin transfer molding) process. Materials with embedded sensors are known as "smart" materials.
- Composite materials have a high specific stiffness (stiffness-to-density ratio). Composites offer the stiffness of steel at one fifth the weight and equal the stiffness of aluminum at one half the weights.
- The specific strength (strength-to-density ratio) of a composite material is very high. Due to this, airplanes and automobiles move faster and with better fuel efficiency. The specific strength is typically in the range of 3 to 5 times that of steel

and aluminum alloys. Due to this higher specific stiffness and strength, composite parts are lighter than their counterparts.

- The fatigue strength (endurance limit) is much higher for composite materials. Steel and aluminum alloys exhibit good fatigue strength up to about 50% of their static strength. Unidirectional carbon/epoxy composites have good fatigue strength up to almost 90% of their static strength.

- Composite materials offer high corrosion resistance. Iron and aluminum corrode in the presence of water and air and require special coatings and alloying. Because the outer surface of composites is formed by plastics, corrosion and chemical resistance are very good.

- Composite materials offer increased amounts of design flexibility. For example, the coefficient of thermal expansion (CTE) of composite structures can be made zero by selecting suitable materials and lay-up sequence. Because the CTE for composites is much lower than for metals, composite structures provide good dimensional stability.

- Net-shape or near-net-shape parts can be produced with composite materials. This feature eliminates several machining operations and thus reduces process cycle time and cost.

- Complex parts, appearance, and special contours, which are sometimes not possible with metals, can be fabricated using composite materials without welding or riveting the separate pieces. This increases reliability and reduces production times. It offers greater manufacturing feasibility.

- Composite materials offer greater feasibility for employing design for manufacturing (DFM) and design for assembly (DFA) techniques. These techniques help minimize the number of parts in a product and thus reduce assembly and joining time. By eliminating joints, high-strength structural parts can be manufactured at lower cost. Cost benefit comes by reducing the assembly time and cost.

- Composites offer good impact properties, as shown in Figures 2.7 and 2.8. Figure 2.7 shows impact properties of aluminum, steel, glass/epoxy, kevlar/epoxy, and carbon/epoxy continuous fiber composites. Glass and Kevlar composites provide higher impact strength than steel and aluminum. Figure 2.8 compares impact properties of short and long glass fiber thermoplastic composites with aluminum and magnesium. Among thermoplastic composites, impact properties of long glass fiber

nylon 66 composite (NylonLG60) with 60% fiber content, short glass fiber nylon 66 composite (NylonSG40) with 40% fiber content, long glass fiber polypropylene composite (PPLG40) with 40% fiber content, short

▪ Glass fiber polypropylene composite (PPSG40) with 40% fiber content, long glass fiber PPS composite (PPSLG50) with 50% fiber content, and long glass fiber polyurethane composite (PULG60) with 60% fiber content are described. Long glass fiber provides three to four times improved impact properties than short glass fiber composites.

▪ Noise, vibration, and harshness (NVH) characteristics are better for composite materials than metals. Composite materials dampen vibrations an order of magnitude better than metals. These characteristics are used in a variety of applications, from the leading edge of an airplane to golf clubs.

▪ By utilizing proper design and manufacturing techniques, cost-effective composite parts can be manufactured. Composites offer design freedom by tailoring material properties to meet performance specifications, thus avoiding the over-design of products. This is achieved by changing the fiber orientation, fiber type, and/or resin systems.
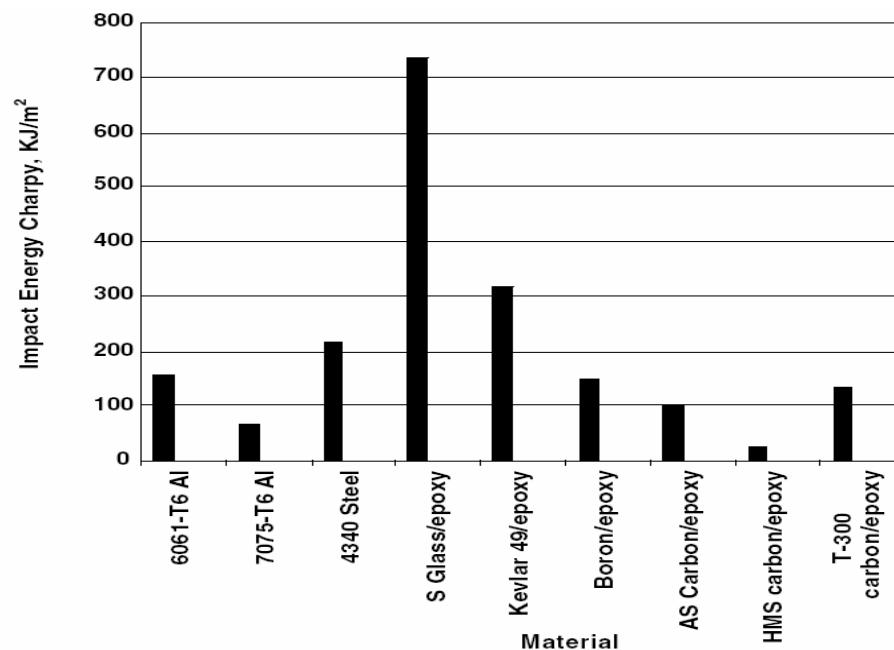

Figure 2.7 Impact properties of various engineering materials. unidirectional composite materials with about 60% fiber volume fraction are used.
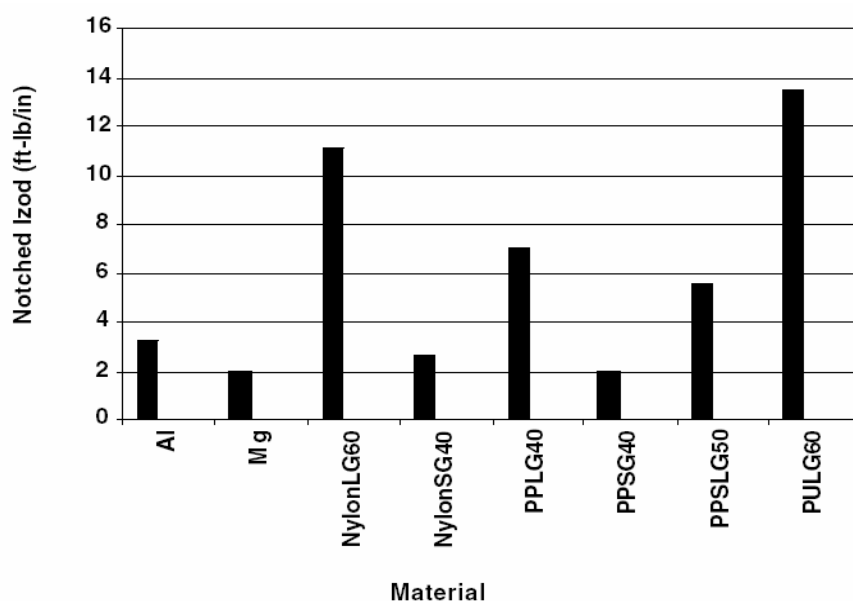
Figure 2.8 Impact properties of long glass (LG) and short glass (SG) fibers reinforced thermoplastic composites. fiber weight percent is written at the end in two digits.

- Glass-reinforced and aramid-reinforced phenolic composites meet FAA and JAR requirements for low smoke and toxicity. This feature is required for aircraft interior panels, stow bins, and galley walls.

- The cost of tooling required for composites processing is much lower than that for metals processing because of lower pressure and temperature requirements. This offers greater flexibility for design changes in this competitive market where product lifetime is continuously reducing.

2.6 Drawbacks of Composites

Although composite materials offer many benefits, they suffer from the following disadvantages:

- The materials cost for composite materials is very high compared to that of steel and aluminum. It is almost 5 to 20 times more than aluminum and steel on a weight basis. For example, glass fiber costs $1.00 to $8.00/lb; carbon fiber costs $8 to $40/lb; epoxy costs $1.50/lb; glass/epoxy prepreg costs $12/lb; and carbon/epoxy prepreg costs $12 to $60/lb. The cost of steel is $0.20 to $1.00/lb and that of aluminum is $0.60 to $1.00/lb.

▪ In the past, composite materials have been used for the fabrication of large structures at low volume (one to three parts per day). The lack of high-volume production methods limits the widespread use of composite materials. Recently, pultrusion, resin transfer molding (RTM), structural reaction injection molding (SRIM), compression molding of sheet molding compound (SMC), and filament winding have been automated for higher reduction rates. Automotive parts require the production of 100 to 20,000 parts per day. For example, Corvette volume is 100 vehicles per day, and Ford-Taurus volume is 2000 vehicles per day.

▪ Steering system companies such as Delphi Saginaw Steering Systems and TRW produce more than 20,000 steering systems per day for various models. Sporting good items such as golf shafts are produced on the order of 10,000 pieces per day.

▪ Classical ways of designing products with metals depend on the use of machinery and metals handbooks, and design and data handbooks. Large design databases are available for metals. Designing parts with composites lacks such books because of the lack of a database.

▪ The temperature resistance of composite parts depends on the temperature resistance of the matrix materials. Because a large proportion of composites uses polymer-based matrices, temperature resistance is limited by the plastics' properties. Average composites work in the temperature range –40 to +100°C. The upper temperature limit can range between +150 and +200°C for high temperature plastics such as epoxies, bismaleimides, and PEEK. Table 2.2 shows the maximum continuous-use temperature for various polymers.

▪ Solvent resistance, chemical resistance, and environmental stress cracking of composites depend on the properties of polymers. Some polymers have low resistance to solvents and environmental stress cracking.

▪ Composites absorb moisture, which affects the properties and dimensional stability of the composites.

Table 2.2 Maximum continuous-use temperatures for various thermosets and thermoplastics

Materials	Maximum Continuous-Use Temperature (°C)
Thermosets	
Vinylester	60–150
Polyester	60–150
Phenolics	70–150
Epoxy	80–215
Cyanate esters	150–250
Bismaleimide	230–320
Thermoplastics	
Polyethylene	50–80
Polypropylene	50–75
Acetal	70–95
Nylon	75–100
Polyester	70–120
PPS	120–220
PEEK	120–250
Teflon	200–260

2.7 Laminate Joints in Composite Structures

Composite materials are commonly used in structures that demand a high level of mechanical performance. Their high strength to weight and stiffness to weight ratios has facilitated the development of lighter structures, which often replace conventional metal structures. Due to strength and safety requirements, these applications require joining composites either to composites or to metals (Okutan & Karakuzu, 2002). High stiffness and strengths can be attained for composite laminates. However, these characteristics are quite different from those of ordinary materials to which we often need to fasten composite laminates. Often, the full strength and stiffness characteristics of the laminate

can not be transferred through the joint without a significant weight penalty. Thus, the topic of joints or other fastening devices is critical to the successful use of composite materials (Jones, 1999).

The two major classes of laminate joints are bonded joints as in Figure 2.9 and bolted joints as in Figure 2.10. Often, the two classes are combined, for example, as in the bonded-bolted joint of Figure 2.11. Joints involving composite materials are often bonded because of the natural presence of resin in the composite and are often also bolted for reasons discussed later. Several characteristics of fiber-reinforced composite materials render them more susceptible to joint problems than conventional metals. These characteristics are weakness in in-plane shear, transverse tension, interlaminar shear, and bearing strength relative to the primary assets of a lamina, the strength and stiffness in the fiber direction (Jones, 1999).
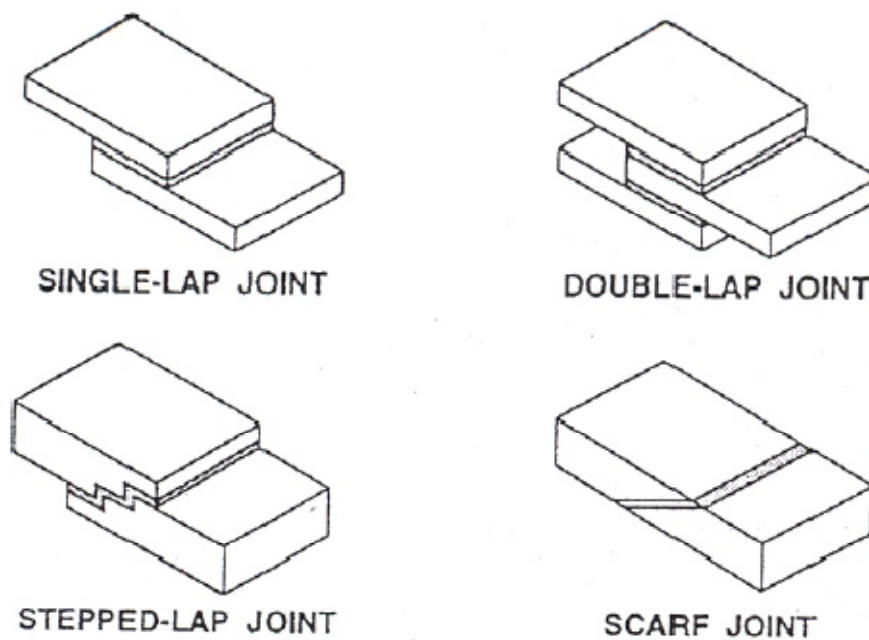

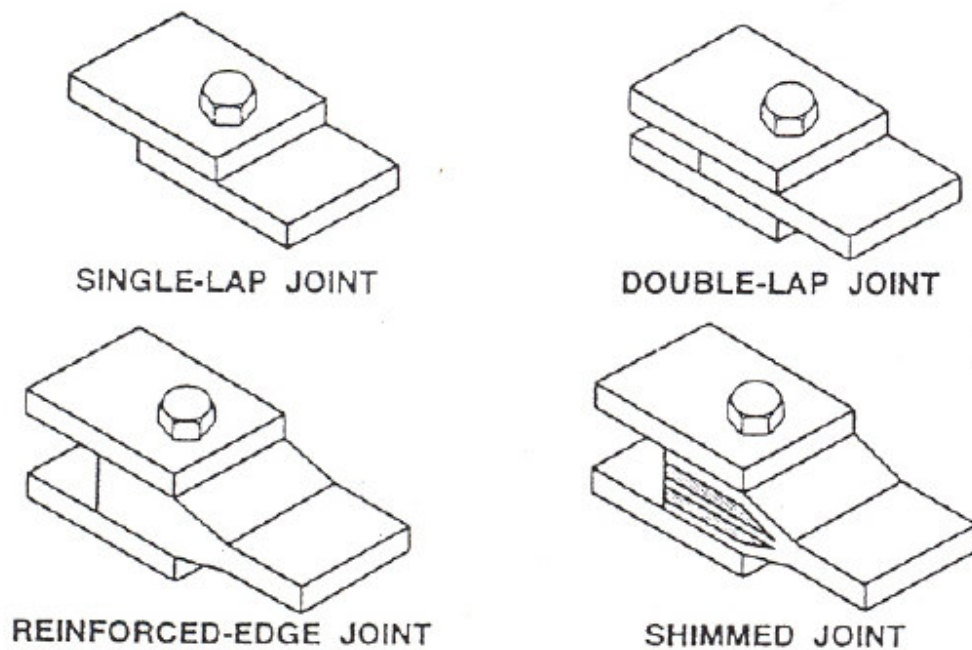Figure 2.9 Bonded joints of composite structures

SINGLE-LAP JOINT   DOUBLE-LAP JOINT

REINFORCED-EDGE JOINT   SHIMMED JOINT

Figure 2.10 Bolted joints of composite structures
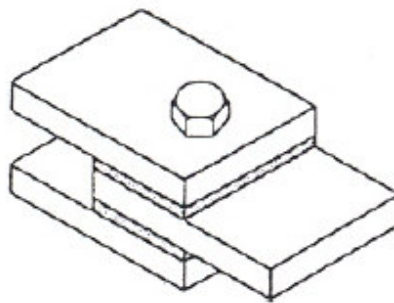

Figure 2.11 Bonded - bolted joints of composite structures

2.7.1 Bonded Joints of Composite Materials

Adhesively bonded joints have been used widely in structures as a result of advancements in adhesive technology. Adhesive bonding allows structural components with different mechanical properties to be joined, such as composite and metal components. Analytical and experimental studies have been concentrated on the stress and deformation states of the adhesive layer and adherents forming the adhesive joint (Apalak et al., 2003). The fundamental design problem in bonded joints is to get enough bond area in shear to carry the load through the joint. Bond area in tension is of little value because of the typically low strength of bonding materials compared to the far higher strength of the metals or composite materials being joined.

2.7.2 Bolted Joints of Composite Materials

Many papers deal with the failure analysis of bolted composite joints. This is mainly due to the fact that joining composite structural components often requires mechanical fasteners which ultimately makes mechanical response difficult to predict. Contrary to many metallic structural parts, for which the strength of the joints is mainly governed by the shear and the tensile strengths of the pins, composite joints present specific failure modes due to their heterogeneity and anisotropy (Pierron et al., 2000). The principal failure modes of bolted joints are (1) bearing failure of the materials as in the elongated bolt hole of Figure 2.12, (2) tension failure of the material in the reduced cross section through the bolt hole, (3) shear-out or cleavage failure of the material (actually transverse tension failure of the material), and (4) bolt failures (mainly shear failures). Of course, combinations of these failures do occur (Jones, 1999).
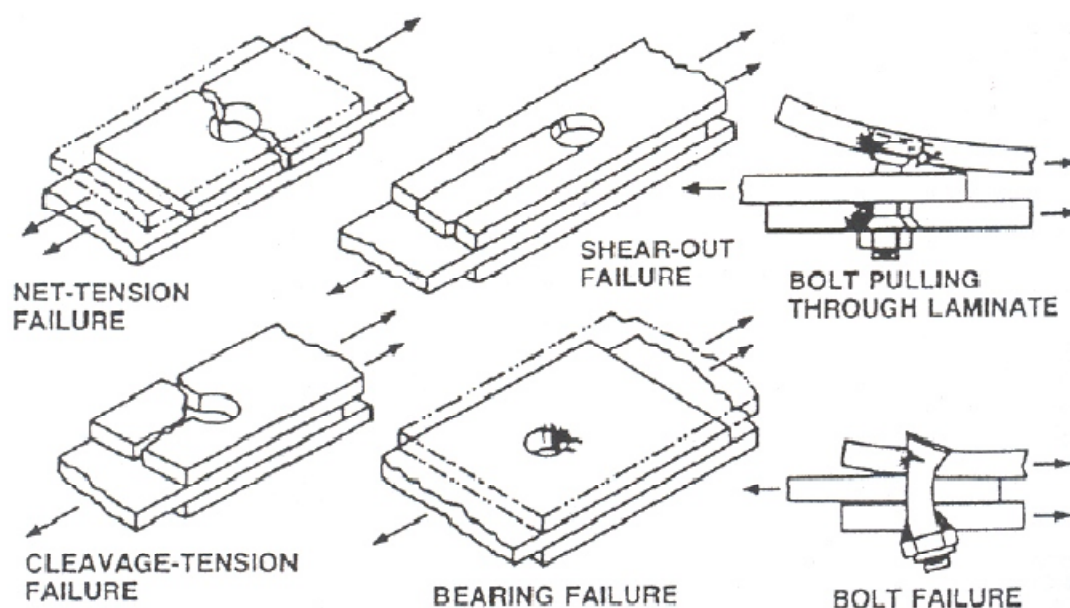

NET-TENSION FAILURE

SHEAR-OUT FAILURE

BOLT PULLING THROUGH LAMINATE

CLEAVAGE-TENSION FAILURE

BEARING FAILURE

BOLT FAILURE

Figure 2.12 Bolted joint failures

2.7.3 Bonded-Bolted Joints of Composite Materials

Bonded-bolted joints generally have better performance than either bonded or bolted joints. The bonding results in reduction of the usual tendency of a bolted joint to shear out. The bolting decreases the likelihood of a bonded joint debonding in an interfacial shear mode. The usual mode of failure for a bonded-bolted joint is either a tension failure through a section including a fastener or an interlaminar shear failure in the

composite material or a combination of both. Bonded-bolted joints have good load distribution and are generally designed so that the bolts take all the loads. Then, the bolts would take all the loads after the bond breaks (because the bolts do not receive load until the bond slips). The bond provides a change in failure mode and a sizeable margin against fatigue failure.

2.7.4 Design of Joints of Composite Materials

It is clear that joints must be considered an integral part of the design process. A structural joint represents a critical element in virtually all hardware designs. In a composite structure, the joint may be made totally or partially of composite materials. The method of joining may be adhesive bonding or mechanical fastening; in many situations the latter method is preferred because of its nonpermanent nature.

The designer is confronted, in many instances, with a decision as to whether to specify a bonded or a bolted joint concept for a given structural attachment. Basic considerations that influence this decision usually include the following (Okutan, 2001):

1. The magnitude of the loading, typically expressed as a force per unit joint width that must be transmitted from one end to the other.
2. The geometrical constraints within which the load transfer must be accomplished.
3. The desired reliability of the joint.
4. Environmental factors in joint operation.
5. A need for repetitive assembly and disassembly.
6. Joint efficiency desired (the strength-weight factor).
7. Cost of manufacture, assembly, and inspection.

In addition, to estimate the strength of single pin-loaded specimens, the static strengths are defined as (Okutan, 2001):

Net-tension Strength: The stress at net-tension section, at failure, is given by:

$$(\sigma_t)_{ult} = \frac{P_{ult}}{(W-D).t} \qquad (2.1)$$

Where P_{ult} is the failing load of the member, W is the joint width at net-section, D is

the hole diameter and t the joint thickness.

Bearing Strength: The bearing strength of a composite material is expressed in the form,

$$(\sigma_b)_{ult} = \frac{P_{ult}}{D.t} \tag{2.2}$$

Shearing Strength: The strength in this case is given as,

$$(\tau_s)_{ult} = \frac{P_{ult}}{2.E.t} \tag{2.3}$$

Where E is the distance (parallel to the load) between the hole center and the free edge, usually known as the edge distance.

The behavior of joint could be influenced by four groups of parameters (Chen et al., 1994; Okutan, 2001).

1. *Material parameters*; fiber types and form, resin type, fiber orientation, laminate, stacking sequence, etc.
2. *Geometry parameters*; specimen width (W) or ratio of width to hole diameter (W/D), edge distance (E) or ratio of the edge distance to hole diameter (E/D), specimen thickness (t), hole size (D), and pitch for multiple joints.
3. *Fastener parameters*; fastener type, fastener size, clamping area and pressure, washer size and hole size and tolerance.
4. *Design parameters*; loading type (tension, compression, fatigue, etc.), loading direction, joint type (single lap, double lap), geometry (pitch, edge distance, hole pattern etc.), environment and failure criteria.

It is clear that, in view of the very large number of variables involved, a complete characterization of joint behavior is impossible. Rather, the approach should be to determine as thoroughly as possible the behavior of basic joints and to hopefully infer the influence of the more important parameters, from which the behavior of joints and materials can be, predicted (Okutan, 2001).

2.8 Composites Markets

There are many reasons for the growth in composite applications, but the primary impetus is that the products fabricated by composites are stronger and lighter. Today, it is difficult to find any industry that does not utilize the benefits of composite materials. The largest user of composite materials today is the transportation industry, having consumed 1.3 billion pounds of composites in 2000. Composite materials have become the materials of choice for several industries.

In the past three to four decades, there have been substantial changes in technology and its requirement. This changing environment created many new needs and opportunities, which are only possible with the advances in new materials and their associated manufacturing technology.

In the past decade, several advanced manufacturing technology and material systems have been developed to meet the requirements of the various market segments. Several industries have capitalized on the benefits of composite materials. The vast expansion of composite usage can be attributed to the decrease in the cost of fibers, as well as the development of automation techniques and high-volume production methods. For example, the price of carbon fiber decreased from $150.00/lb in 1970 to about $8.00/lb in 2000. This decrease in cost was due to the development of low-cost production methods and increased industrial use.

Broadly speaking, the composites market can be divided into the following industry categories: aerospace, automotive, construction, marine, corrosion resistant equipment, consumer products, appliance/business equipment, and others. U.S. composite shipments in the above markets are shown in Figure 2.13 for the years 1999 and 2000 (projected).
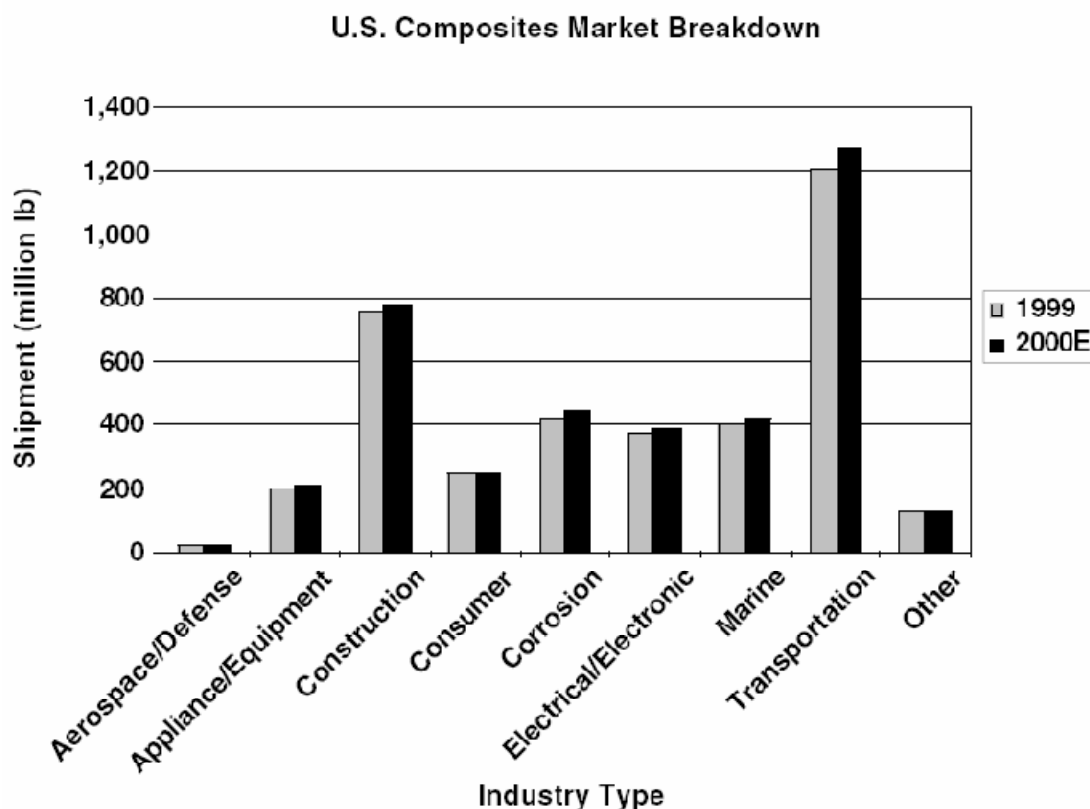
U.S. Composites Market Breakdown

Figure 2.13 Composite shipments in various industries in 1999 and those projected for 2000.

2.8.1 The Aerospace Industry

The aerospace industry was among the first to realize the benefits of composite materials. Airplanes, rockets, and missiles all fly higher, faster, and farther with the help of composites. Glass, carbon, and Kevlar fiber composites have been routinely designed and manufactured for aerospace parts. The aerospace industry primarily uses carbon fiber composites because of their high-performance characteristics. The hand lay-up technique is a common manufacturing method for the fabrication of aerospace parts; RTM and filament winding are also being used.

In 1999, the aerospace industry consumed 23 million pounds of composites, as shown in Figure 2.14. Military aircrafts, such as the F-11, F-14, F-15, and F-16, use composite materials to lower the weight of the structure. The composite components used in the above-mentioned fighter planes are horizontal and vertical stabilizers, wing skins, fin boxes, flaps, and various other structural components as shown in Table 2.3. Typical
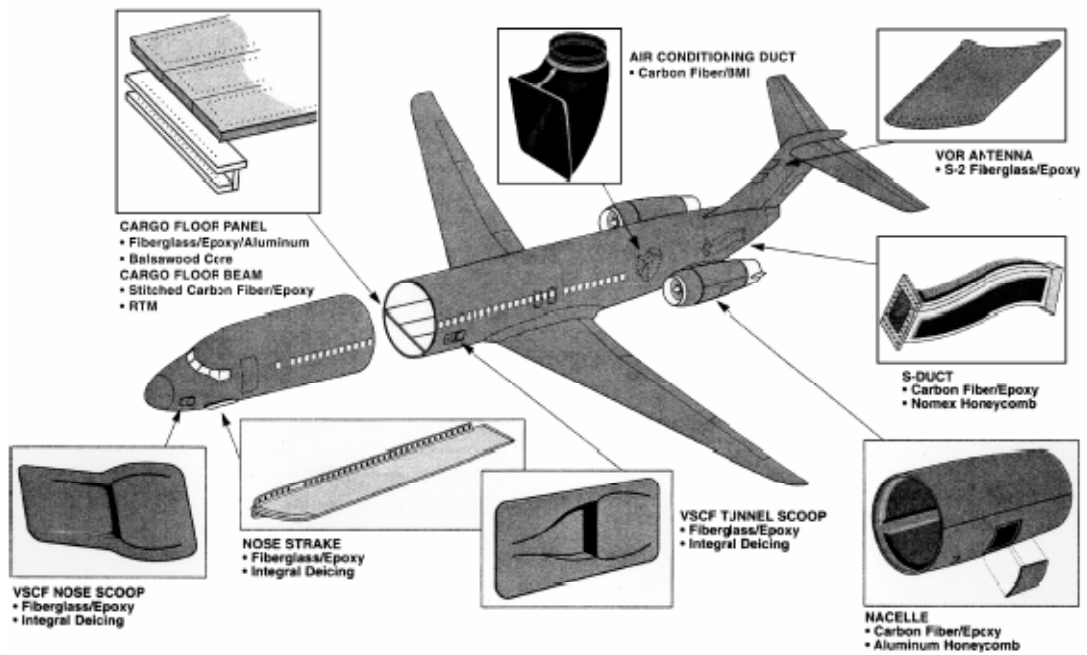
mass reductions achieved for the above components are in the range of 20 to 35%. The mass saving in fighter planes increases the payload capacity as well as the missile range.

Figure 2.14.a, Figure 2.14.b and Figure 2.14.c show the typical composite structures used in commercial aircraft and Figure 2.15.a and Figure 2.15.b shows the typical composite structures used in military aircraft. Composite components used in engine and satellite applications are shown in Figures 2.16 and 2.17, respectively.
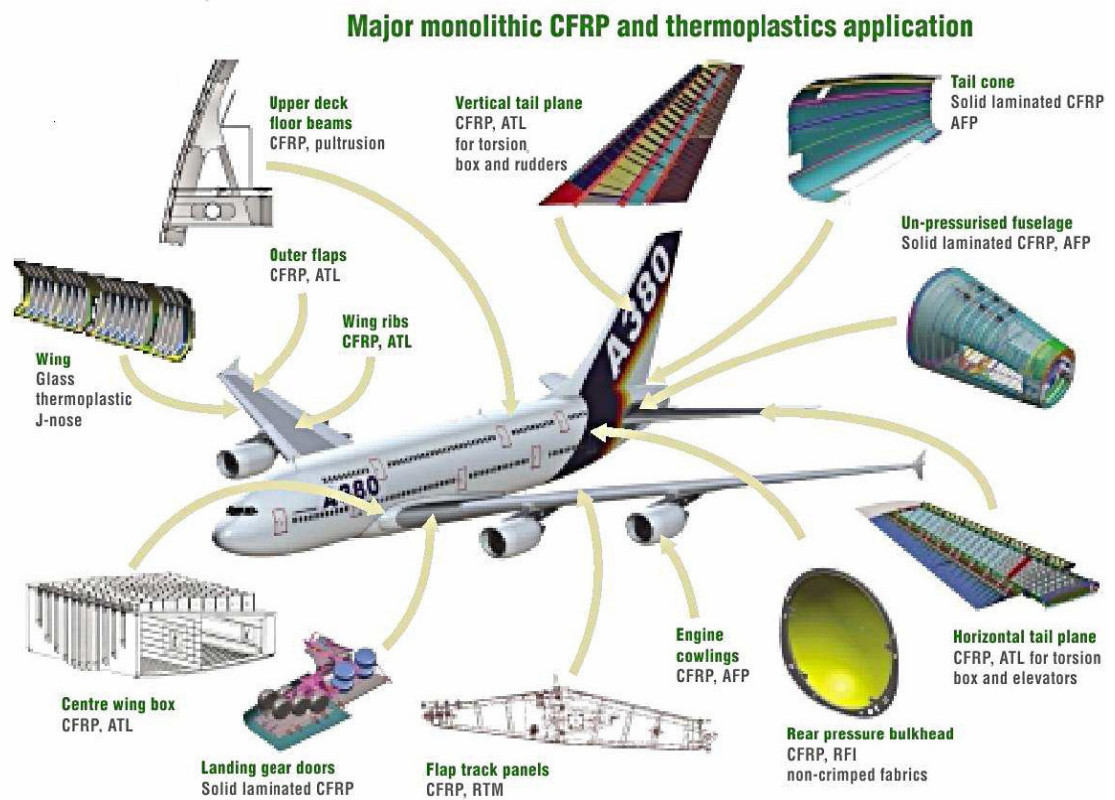
Table 2.3 Composite components in aircraft applications

Composite Components	
F-14	Doors, horizontal tails, fairings, stabilizer skins
F-15	Fins, rudders, vertical tails, horizontal tails, speed brakes, stabilizer skins
F-16	Vertical and horizontal tails, fin leading edge, skins on vertical fin box
B-1	Doors, vertical and horizontal tails, flaps, slats, inlets
AV-8B	Doors, rudders, vertical and horizontal tails, ailerons, flaps, fin box, fairings
Boeing 737	Spoilers, horizontal stabilizers, wings
Boeing 757	Doors, rudders, elevators, ailerons, spoilers, flaps, fairings
Boeing 767	Doors, rudders, elevators, ailerons, spoilers, fairings

Commercial Aircraft
Composite Structures

AIR CONDITIONING DUCT
• Carbon Fiber/BMI

VOR ANTENNA
• S-2 Fiberglass/Epoxy

CARGO FLOOR PANEL
• Fiberglass/Epoxy/Aluminum
• Balsawood Core
CARGO FLOOR BEAM
• Stitched Carbon Fiber/Epoxy
• RTM

S-DUCT
• Carbon Fiber/Epoxy
• Nomex Honeycomb

NOSE STRAKE
• Fiberglass/Epoxy
• Integral Deicing

VSCF TJNNEL SCOOP
• Fiberglass/Epoxy
• Integral Deicing

VSCF NOSE SCOOP
• Fiberglass/Epoxy
• Integral Deicing

NACELLE
• Carbon Fiber/Epcxy
• Aluminum Honeycomb

(a)

Major monolithic CFRP and thermoplastics application
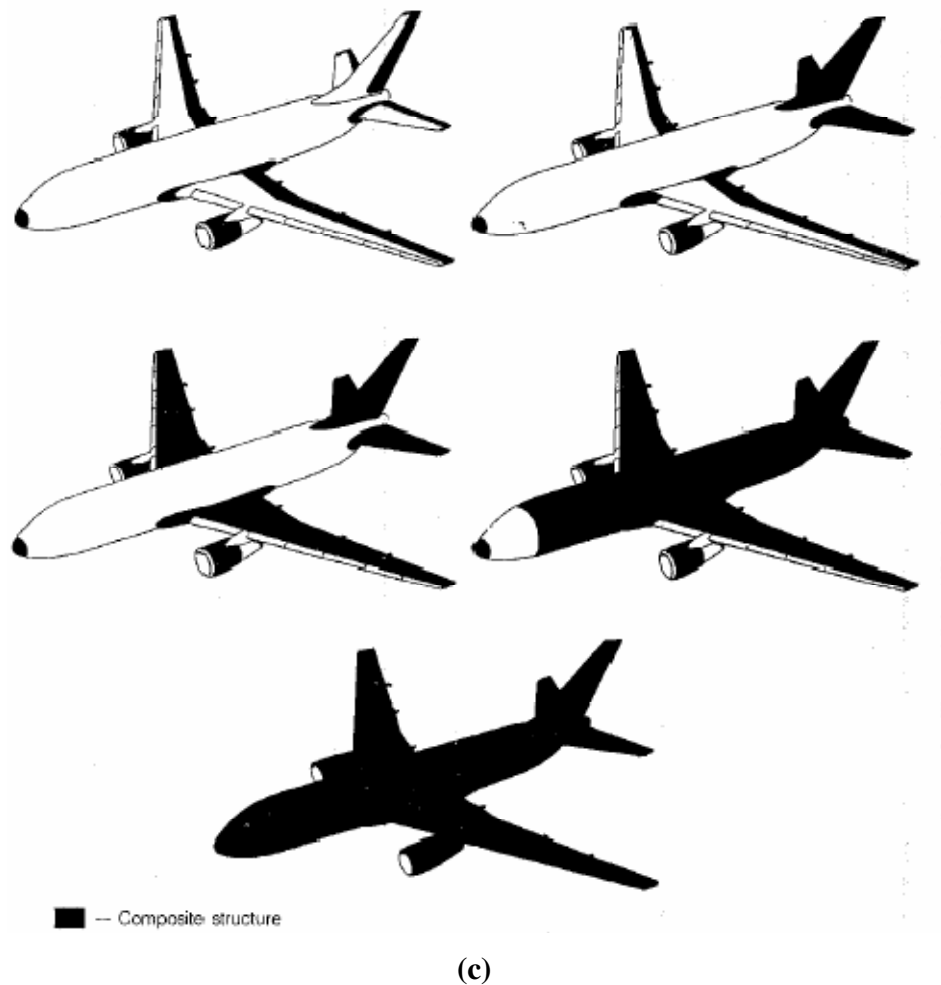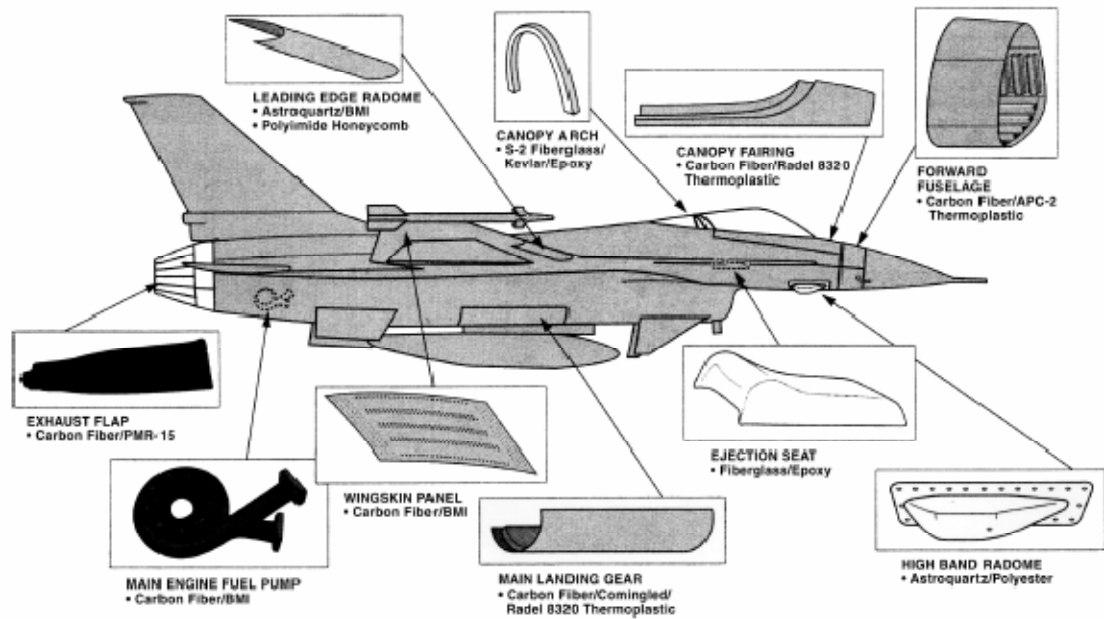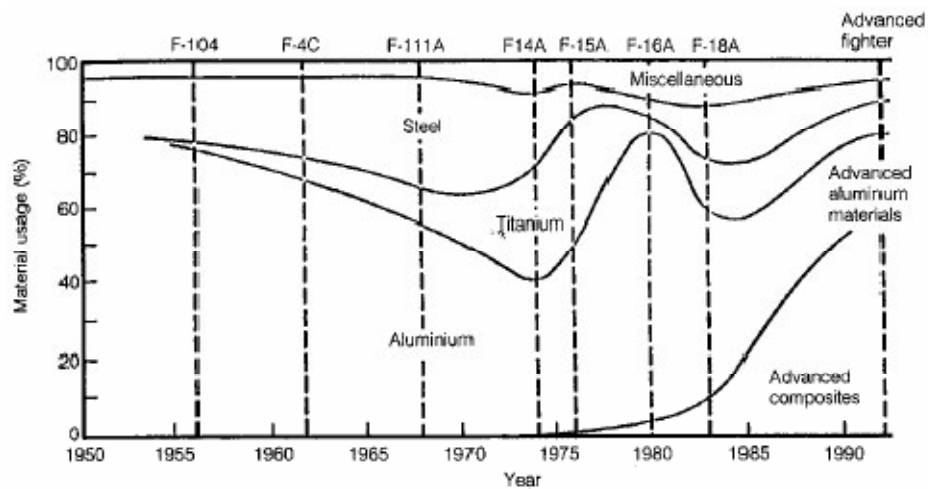
(b)

(c)

Figure 2.14 **a)** typical composite structures used in commercial aircraft. **b)** Major composite parts on the Airbus A380 **c)** The progressive use of composites on commercial transport airframes

The major reasons for the use of composite materials in spacecraft applications include weight savings as well as dimensional stability. In low Earth orbit (LEO), where temperature variation is from –100 to +100°C, it is important to maintain dimensional stability in support structures as well as in reflecting members. Carbon epoxy composite laminates can be designed to give a zero coefficient of thermal expansion. Typical space structures are tubular truss structures, face sheets for the payload bay door, antenna reflectors, etc. In space shuttle composite materials provide weight savings of 2688 lb per vehicle.

Military Aircraft
Composite Structures

LEADING EDGE RADOME
• Astroquartz/BMI
• Polyimide Honeycomb

CANOPY ARCH
• S-2 Fiberglass/
  Kevlar/Epoxy

CANOPY FAIRING
• Carbon Fiber/Radel 8320
  Thermoplastic

FORWARD FUSELAGE
• Carbon Fiber/APC-2
  Thermoplastic

EXHAUST FLAP
• Carbon Fiber/PMR-15

MAIN ENGINE FUEL PUMP
• Carbon Fiber/BMI

WINGSKIN PANEL
• Carbon Fiber/BMI

MAIN LANDING GEAR
• Carbon Fiber/Comingled/
  Radel 8320 Thermoplastic

EJECTION SEAT
• Fiberglass/Epoxy

HIGH BAND RADOME
• Astroquartz/Polyester

(a)

(b)

Figure 2.15 **a)** Typical composite structures used in military aircraft **b)** Progress in using composite materials on military fighter aircraft
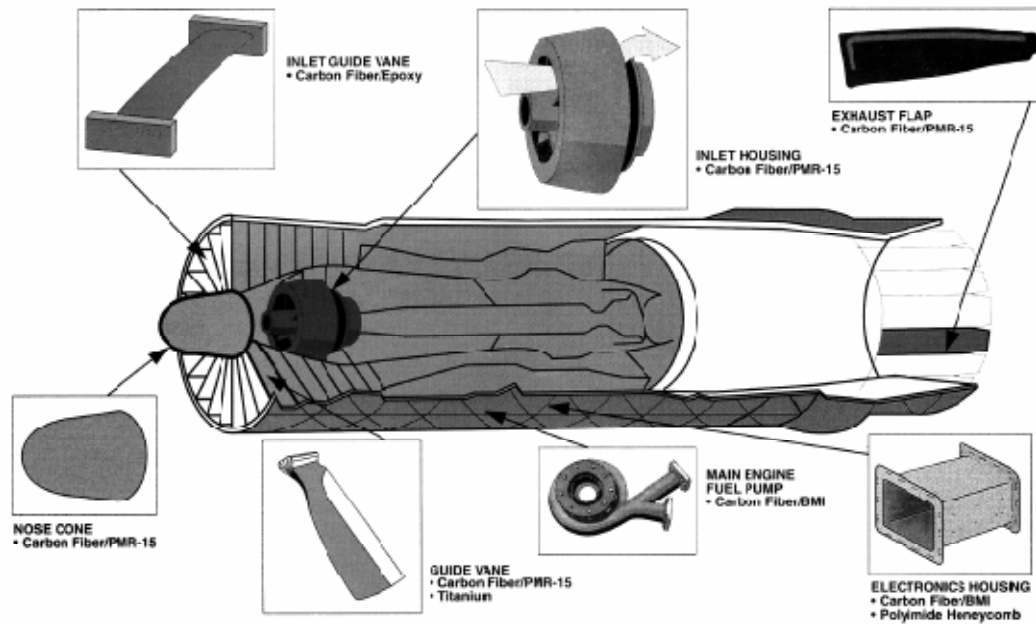
Engine Components

Figure 2.16 Composite components used in engine applications
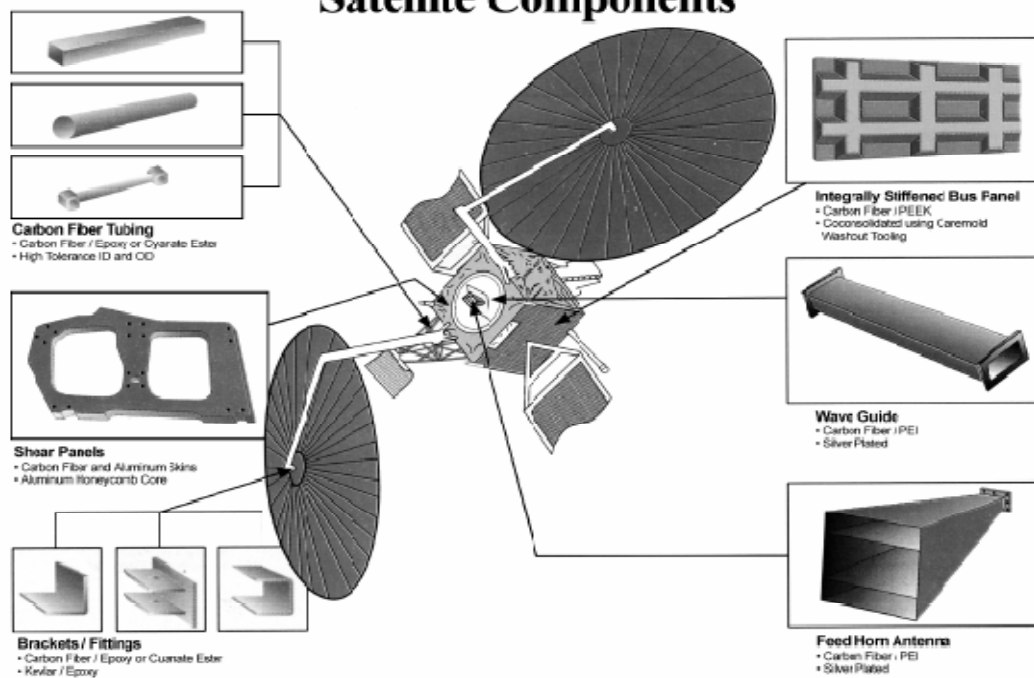
Satellite Components

Figure 2.17 Composite components used in satellite applications

Passenger aircrafts such as the Boeing 747 and 767 use composite parts to lower the weight, increase the payload, and increase the fuel efficiency. The components made out of composites for such aircrafts are shown in Table 2.4

2.8.2 The Automotive Industry

Composite materials have been considered the "material of choice" in some applications of the automotive industry by delivering high-quality surface finish, styling details, and processing options. Manufacturers are able to meet automotive requirements of cost, appearance, and performance utilizing composites. Today, composite body panels have a successful track record in all categories — from exotic sports cars to passenger cars to small, medium, and heavy truck applications. In 2000, the automotive industry used 318 million pounds of composites.

Because the automotive market is very cost-sensitive, carbon fiber composites are not yet accepted due to their higher material costs. Automotive composites utilize glass fibers as main reinforcements. Table 2.4 provides a breakdown of automotive composite usage by applications, matrix materials, and manufacturing methods.

Figure 2.18 Composite applications in automotive industry

Table 2.4 Average uses of composites in automobiles per year, 1988-1993

Applications	Usage (kg x 106)	Matrix Material	Usage (kg x 106)	Manufacturing Process	Usage (kg x 106
Bumper beam	42	Polyester (TS)	42	SMC (comp. mold	40
Seat/load floor	14	Polypropylene	22	GMT (comp. mold)	20
Hood	13	Polycarbonate/PBT	10	Injection molding	13
Radiator support	4	Polyethylene	4	Ext. blow mold	5
Roof panel	4	Epoxy	4	Filament wound	3
Other	11	Other	7	Other	8
Total	89	Total	89	Total	89

2.8.3 The Sporting Goods Industry

Sports and recreation equipment suppliers are becoming major users of composite materials. The growth in structural composite usage has been greatest in high performance sporting goods and racing boats. Anyone who has visited a sporting goods store can see products such as golf shafts, tennis rackets, snow skis, fishing rods, etc. made of composite materials. These products are light in weight and provide higher performance, which helps the user in easy handling and increased comfort.

2.8.4 Marine Applications

Composite materials are used in a variety of marine applications such as passenger ferries, power boats, buoys, etc. because of their corrosion resistance and light weight, which gets translated into fuel efficiency, higher cruising speed, and portability. The majority of components is made of glass-reinforced plastics (GRP) with foam and honeycomb as core materials. About 70% of all recreational boats are made of composite materials according to a 361-page market report on the marine industry. According to this report total annual domestic boat shipments in the United States was

$8.85 billion and total composite shipments in the boating industry worldwide is estimated as 620 million lbs in 2000.

Composites are also used in offshore pipelines for oil and gas extractions. The motivation for the use of GRP materials for such applications includes reduced handling and installation costs as well as better corrosion resistance and mechanical performance. Another benefit comes from the use of adhesive bonding, which minimizes the need for a hot work permit if welding is employed.

2.8.5 Consumer Goods

Composite materials are used for a wide variety of consumer good applications, such as sewing machines, doors, bathtubs, tables, chairs, computers, printers, etc. The majority of these components are short fiber composites made by molding technology such as compression molding, injection molding, RTM, and SRIM.

2.8.6 Construction and Civil Structures

The construction and civil structure industries are the second major users of composite materials. Construction engineering experts and engineers agree that the U.S. infrastructure is in bad shape, particularly the highway bridges. Some 42% of this nation's bridges need repair and are considered obsolete, according to Federal Highway Administration officials. The federal government has budgeted approximately $78 billion over the next 20 years for major infrastructure rehabilitation. The driving force for the use of glass-and carbon-reinforced plastics for bridge applications is reduced installation, handling, repair, and life-cycle costs as well as improved corrosion and durability. It also saves a significant amount of time for repair and installation and thus minimizes the blockage of traffic. Composite usage in earthquake and seismic retrofit activities is also booming. The columns wrapped by glass/epoxy, carbon/epoxy, and aramid/epoxy show good potential for these applications.

2.8.7 Industrial Applications

The use of composite materials in various industrial applications is growing. Composites are being used in making industrial rollers and shafts for the printing industry and industrial drive shafts for cooling-tower applications. Filament winding

shows good potential for the above applications. Injection molded, short fiber composites are used in bushings, pump and roller bearings, and pistons. Composites are also used for making robot arms and provide improved stiffness, damping, and response time.

2.9 Barriers in Composite Markets

The primary barrier to the use of composite materials is their high initial costs in some cases, as compared to traditional materials. Regardless of how effective the material will be over its life cycle, industry considers high upfront costs, particularly when the life-cycle cost is relatively uncertain. This cost barrier inhibits research into new materials. In general, the cost of processing composites is high, especially in the hand lay-up process. Here, raw material costs represent a small fraction of the total cost of a finished product. There is already evidence of work moving to Asia, Mexico, and Korea for the cases where labor costs are a significant portion of the total product costs. The recycling of composite materials presents a problem when penetrating a high-volume market such as the automotive industry, where volume production is in the millions of parts per year. With the new government regulations and environmental awareness, the use of composites has become a concern and poses a big challenge for recycling. (Matthews et al., 2000), (Mazumdar, 2002).

CHAPTER THREE

MEASUREMENT OF BASIC MATERIAL PROPERTIES

3.1 Introduction

The purpose of this chapter is to review briefly the most used methods for mechanical testing of composite materials and their constituents. Much of our knowledge about the special nature of composite behavior has been derived from experimental observations. The measurement of mechanical properties is also an important element of the quality control and quality assurance processes associated with the manufacture of composite materials and structures. Due to the special characteristics of composites, such as anisotropy, coupling effects and the variety of possible failure modes, it has been found that the mechanical test methods that are used for conventional metallic materials are usually not applicable to composites. Thus, the development and evaluation of new test methods for composites has been, and continues to be, a major challenge for the experimental mechanics community. The technology associated with composite test methods and test equipment has become just as sophisticated as that associated with the corresponding analytical methods. Many of these test methods have evolved into standards which have been adopted by the American Society for Testing and Materials (ASTM) (Gibson, 1994).

Nine independent elastic constants are required to define the mechanical response of an orthotropic lamina (Staab, 1999). The determination of basic material properties of unidirectional laminated composite plate under static loading conditions using experimental method has always been a key issue in the research on composite materials. With the rise of huge variety of composites, the need for an efficient and reliable way of measuring these properties has become more important. The experiments, if conducted properly, generally reveal both strengths and stiffness characteristics of the material (Okutan, 2001).

The strengths characteristics are;

X : Axial or longitudinal strength (1 direction)

Y : Transverse strength (2 direction)

S : Shear strength (1-2 plane)

The stiffness characteristics are;

E_1, E_2 : Longitudinal and transverse Young modulus

v_{12} : Poisson's ratio

G_{12} : Shear modulus

3.2 Experimental Process

It will be considered the mechanics of materials approach in describing fiber-matrix interactions in a unidirectional lamina owing to tensile and compressive loadings. The basic assumptions in this vastly simplified approach are as follows (Mallick, 1993):

1. Fibers are uniformly distributed throughout the matrix.
2. Perfect bonding exists between fibers and matrix.
3. The matrix is free of voids.
4. Applied loads are either parallel to or normal to the fiber direction.
5. The lamina is initially in a stress-free state (i.e., no residual stresses are present)
6. Both fibers and matrix behave as linearly elastic materials.

Experiments are carried out using SHIMADZU Test Machine in Composite Laboratory at Dokuz Eylul University, Figure 3.1.
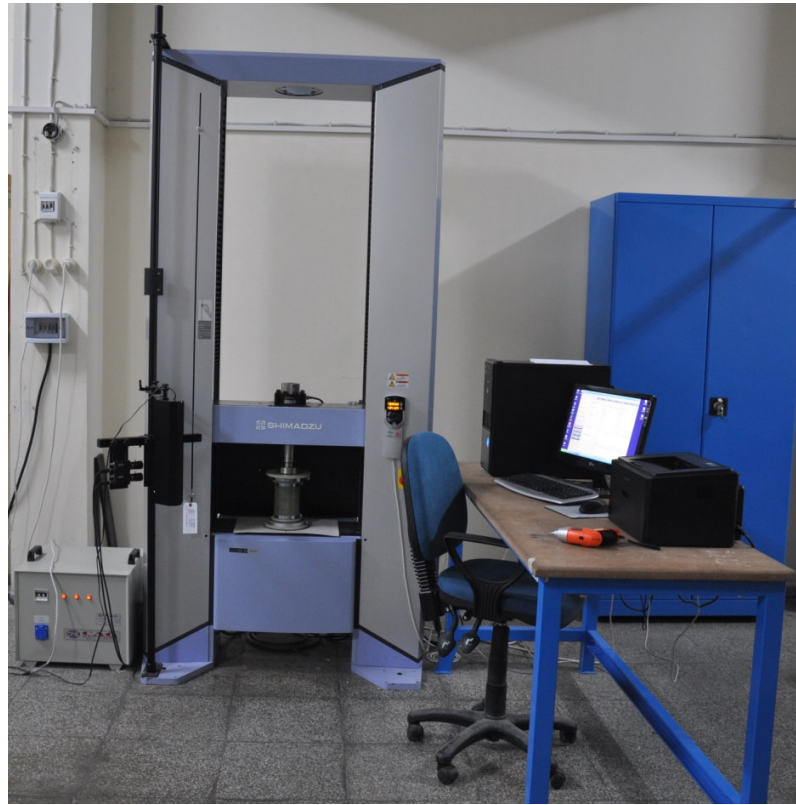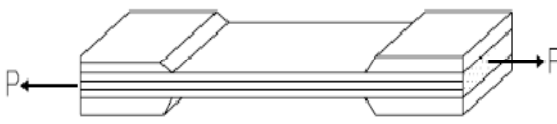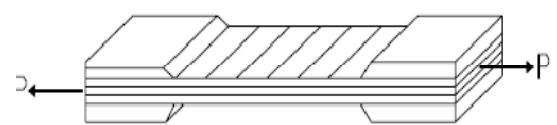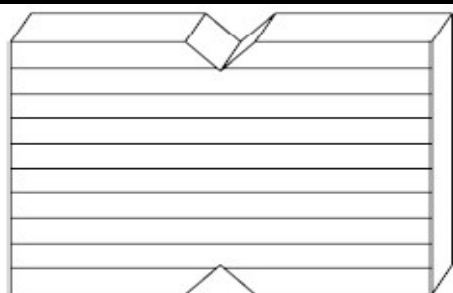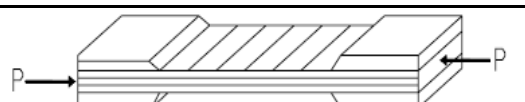
Figure 3.1 A view of the SHIMADZU test machine

A personal computer and two digital cameras are also linked to this testing machine for data acquisition. Applied load and displacement are monitored for static experiments. In addition, the strain is also measured by using strain gages. The geometries and standards of the test specimen are illustrated in Table 3.1 (Gibson, 1994; Jones, 1999; Okutan, 2001).

The required basic material properties are estimated under three primary loading modes that are tension, compression and in-plane shear.

Table 3.1 Geometries of the experiment specimens

Determinable Properties	Symbol and Unit	ASTM Test Method	Specimen Geometry
Axial or longitudinal modulus	E_1 (MPa)	ASTM 3039-76	
Axial Poisson's ratio	ν_{12} (-)		
Longitudinal tensile strength	X_t (MPa)		
Transverse modulus	E_2 (MPa)	ASTM 3039-76	
Transverse tensile strength	Yt (MPa)		
Shear modulus	G_{12} (MPa)	ASTM D 7078	
Shear Strength	S (MPa)		
Longitudinal compressive strength	X_C (MPa)	ASTM 3410-75	
Transverse compressive strength	Y_C (MPa)	ASTM 3410-75	

3.2.1 Measurement of the Tensile Properties

Tensile properties of glass-epoxy laminated composite plate such as Longitudinal Young's modulus E_1, longitudinal tensile strengths X_t, Poisson's ratio v_{12}, transverse Young's modulus E_2, and transverse tensile strengths Y_t were measured by using longitudinal $[0]_8$ and transverse $[90]_8$ unidirectional composite specimens in accordance with the ASTM D3039-76 standard. The test specimens were loaded until failure occurred in the axial and transverse directions. Young's moduli of E_1 and E_2 were calculated by the tensile machine by using two digital cameras which were mounted on

the machine for measuring the variations in longitudinal axis of the machine using the initial slope of the stress–strain curves for these calculations. The tensile strengths of the unidirectional composite plates, X_t and Y_t, were determined by dividing the failure load to the cross sectional area of the longitudinal and transverse specimens, respectively. Poisson's ratio v_{12} was measured using the strain gages that bonded at the center of the test specimen. These are considered at the following sections.

The tensile test specimen is straight sided and has a constant cross-section. As illustrated in figure 3.2, the tensile test geometry to find the longitudinal tensile properties consist of eighth laminas. The laminas were positioned $[0°]_8$ orientation 13 mm wide and 250 mm length.
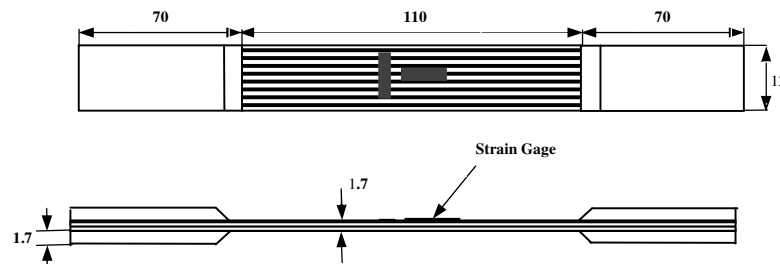

Figure 3.2 The dimensions and geometry of longitudinal tensile test specimen

The tensile specimen is positioned in the testing machine, taking care to align the longitudinal axis of the specimen and pulled at a cross-head speed of 1 mm/min. The specimens are loaded step by step up to failure under uni-axial tensile loading.

Figure 3.3 Deformed tensile test specimens to obtain longitudinal elasticity module (E_1) and poisson ratio ($\mathcal{V}_{12}$)

A continuous record of load and deflection is obtained by a digital data acquisition system. Axial strain is measured by means of two digital cameras that installed on the test machine and measured variation of displacement at the axial direction of test machine. The stress in the longitudinal direction is drawn as a function of longitudinal strain. The stress-strain behavior is occurred linear and final failure is occurred catastrophically. The magnitudes of E_1, v_{12} and X_t are calculated using the tension test data and Equation (3.1).

$$\sigma_i = E_i \varepsilon_i$$

$$\sigma_1 = \frac{P}{A} \Rightarrow E_1 = \frac{\sigma_1}{\varepsilon_1}$$

$$v_{12} = -\frac{\varepsilon_2}{\varepsilon_1} \tag{3.1}$$

$$X_t = \frac{P_{Max}}{A}$$

In which A is the cross-sectional area of the specimen and perpendicular to the applied load. Additionally, the transverse modulus E_2 and transverse tensile strength Y_t are measured from the tension test data of $[90^{\circ}]_8$ unidirectional laminated plate. The test specimen for transverse tension test is prepared according to ASTM 3039-76 standards. The transverse tensile test specimen and dimensions are also illustrated in Figure 4.4.
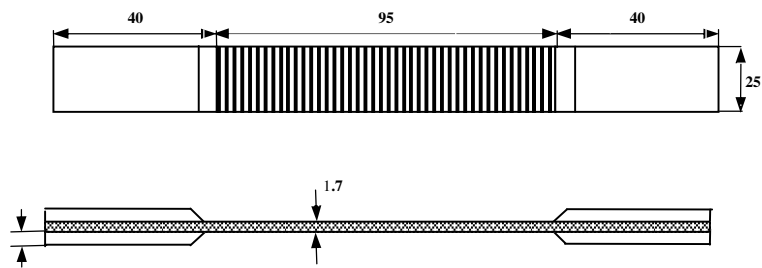
Figure .4 The dimensions and geometry of transverse tensile test specimen

During the measuring process, the specimen is loaded step by step up to break by a machine test and for all steps. The stress-strain behavior is occurred linear and final failure is occurred catastrophically.
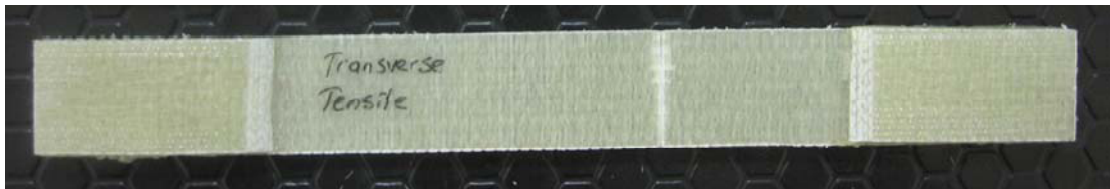

Figure .5. Deformed tensile test specimens to obtain transverse elasticity module (E_2) and transverse tensile strength (Y_t)

The magnitudes of E_2 and Y_t are calculated using the tension test data and Equation (3.2).

$$ \quad\quad (3.2)$$

3.2.2 Measurement of the Compressive Properties

Compression testing of laminated composites is one of the most difficult and interesting types of testing due to sidewise buckling of the test specimen. Many test methods have been developed and used overcome the buckling problem, incorporating variety of test specimen designs and loading fixtures. Even though an ASTM standard for compression testing has been published, there is still much discussion regarding various alternative test methods (Mallick, 1993; Gibson, 1994; Okutan, 2001).

Figure 3.6 A view of compression testing equipment

In this study, the compression properties of the composite laminates were determined experimentally using the Illinois Institute of Technology Research Institute (IITRI) compression test fixture Figure 3.6. The compression test specimens with 140 mm length were prepared according to ASTM D3410 standard. The width was taken as 13 and 25 mm for the longitudinal and transverse specimens, respectively. The longitudinal and transverse compressive strengths, X_c and Y_c, were obtained by dividing the failure

loads to the cross-sectional area of the specimens. The dimensions of the compression test specimens are shown in Figure 3.
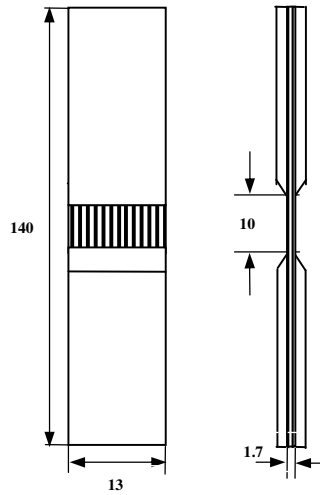

Figure   The dimensions of the compression test specimen

During the experiments, compressive load is performed $[0°]_8$ and $[90°]_8$ glass-epoxy laminated composite specimens. Meanwhile, the maximum failure loads are recorded to obtain longitudinal and transverse compression strengths Xc and Yc.
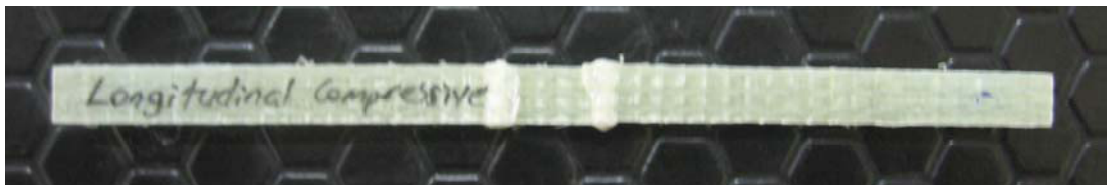

Figure   . Deformed longitudinal compressive test specimens to obtain longitudinal compressive strength (Xc)

Figure   .   Deformed transverse compressive test specimens to obtain transverse compressive strength (Yc)

3.2.3 Measurement of the Shear Properties

As shown earlier, the in plane properties of a composite material are not necessarily equal to the through-thickness shear properties. Thus, test methods which will generate pure shear loading of both types are needed (Gibson, 1994). A variety of test methods have been used for measuring in-plane shear properties, such as the shear modulus G_{12} and the ultimate shear strength τ_{12} of unidirectional fiber reinforced composites (Mallick, 1993).

It is well known that obtaining of shear properties of laminated composites is very difficult types of mechanical static tests. One of the principal difficulties in a development of shear test method for these materials is to induce a stress of pure shear in a gage section of specimen which has to be only subjected to a shear stress of a constant magnitude (Okutan, 2001). There have been many attempts to develop convenient test methods to measure the in-plane shear stress-strain response for composite materials.

The common in-plane shear test methods are;

1. ±45 Shear test

2. 10° Off-axis test

3. Torsion tube

4. Rail shear test

5. Sandwich cross-beam test

6. T-specimen shear

7. Iosipescu shear test

8. V-Notched rail shear test

In this study, V-notched rail shear test (ASTM D 7078) was preferred for measuring the shear modulus and shear strength of composites as it combines the best features of the Iosipescu Shear (ASTM D 5379) and two-rail shear (ASTM D4255) test methods

into a unified test. The 90 degree v-notch configuration of the Iosipescu shear test and the clamped rail configuration of the two-rail shear test have been combined.

A potential problem with the standard Iosipescu shear test method when testing some materials is crushing of the edges of the specimen in the regions where it is loaded by the fixture. The two-rail shear test method utilizes loading rails clamped onto two edges of the specimen by six bolts that pass through holes in the specimen. In addition to the cost and potential specimen damage when preparing these holes, slipping of the specimen in the rails can lead to premature bearing failures as the bolts contact edges of the specimen holes, thus nullifying the test.

The ASTM D 7078 standard specimen is 76 mm long (the same as the standard Iosipescu specimen), but 56mm wide (versus 20 mm for the standard Iosipescu specimen), resulting in a much larger gage section (31 mm wide versus 12 mm). The specimen notch depth to width ratio of 0.225 is nearly the same as the 0.200 for the Iosipescu specimen, thus preserving the gage section geometry.

25mm of each end of the specimen is gripped by the fixture. That is, the specimen is gripped up to the notches, resulting in 26 of specimen being exposed between the grips.

Note in the following photograph the cutout in the lower grip assembly (shown at the left). This is to permit raising the lower grip mounted in the testing machine after the specimen has been installed in the upper grip. This cutout permits installing a specimen without having to remove the fixture from the testing machine, which is sometimes desirable, e.g., when performing elevated temperature or cryogenic tests.

Figure 3.10 V-notched rail shear test equipment

The V-notched rail shear test specimen is tested using this fixture. The strain gauge is installed on the specimen between the notches at 45 degrees as illustrated in Figure 3.11.

Figure 3.11 V-notched rail shear test specimen before tested.

The test specimens are positioned in V-notched rail shear test fixture where the specimen is centered using the alignment pin and lightly clamped with the adjustable wedges as illustrated in Figure 3.12. Afterward the load (P) is carried out to the specimen.
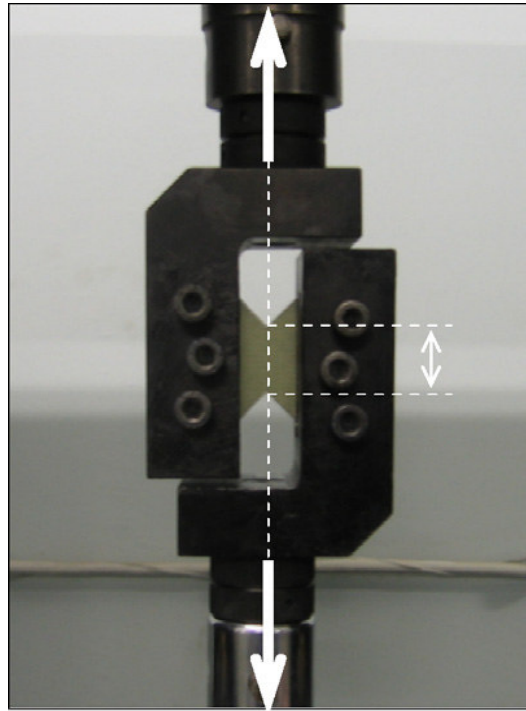
Figure .1   V-notched rail shear test process

During the V-notched rail shear test, SHIMADZU testing machine is used for loading and digital strain meter TDS-530 is used for recorded the strains. The strain-gauge data is recorded and data is reduced to shear strains at the center of the test part and drawn as a function of the applied load. The specimen design and dimensions are illustrated in Figure .1 .
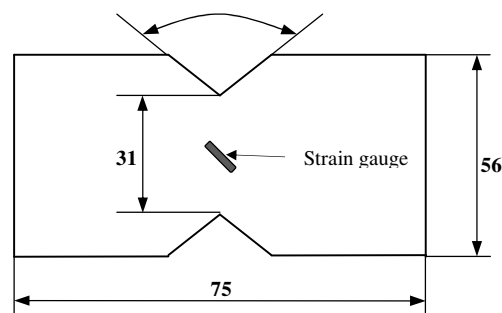

Figure .1   Dimensions of the V-notched rail shear test specimen

According to the V-Notched rail shear test strain-gauges connected to specimens with orientation of $[0]_8$ and $[90]_8$ and shear modules were determined. The strain-gauges which stocked to specimen with 45° angle were connected to the digital strain meter with cables as illustrated Figure .1 .
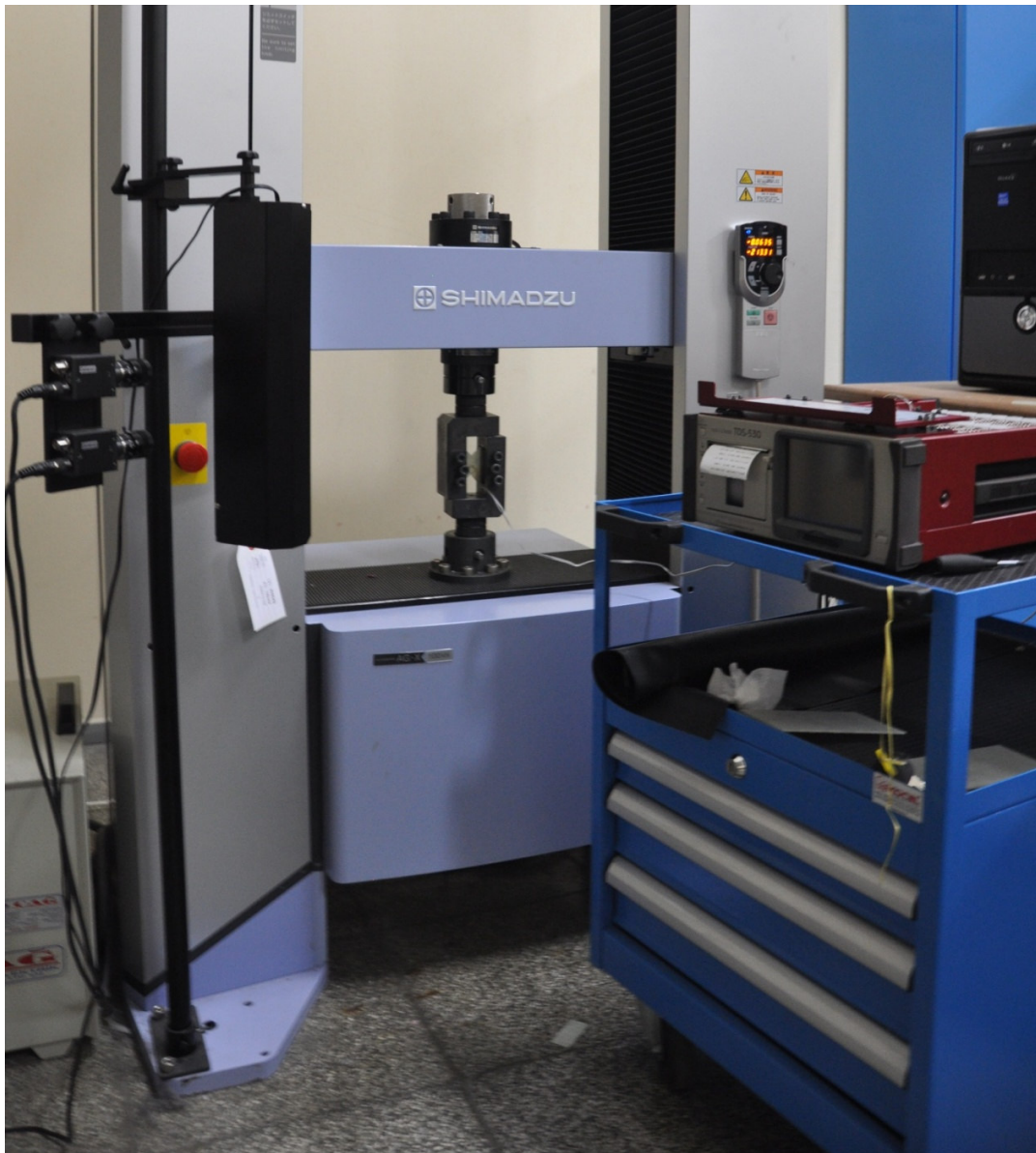
Figure 3.14 Connected indicators to the specimen in V-notched rail shear test process

Test machine was stopped before that the applied load received to the plastic region. It is because of the strains value in the elastic region is more accurate than the plastic region. Force values were written down from computer screen and strain values were written down from strain mater. Then excel table were prepared by written down force and strain values.

Shear module were determined for every point by means of formulas given 4.3. The main shear modules were calculated by averaging determined shear modules.

The in-plane shear strength S_{12} was calculated by:

$$S_{12} = \frac{P_{max}}{wt} \tag{3.3}$$

Where P_{max} is the failure load, w is the width of the specimen at notch location and t is the specimen thickness. Shear modulus G_{12} was measured by using a strain-gauge located at the center of the notched section at 45^0 to the loading direction. Shear stress τ_{12} was obtained by using Equation (1). The shear modulus was calculated by using the following equation;

$$\tau_{12} = G_{12} \cdot \gamma_{12}$$

$$\gamma_{12} = 2.\varepsilon \tag{3.4}$$

$$G_{12} = \frac{P}{2.\varepsilon.w.t}$$

The experimental results of tensile, and compressive, and in-plane shear tests are illustrated in Table 3.2.

Table 3.2 Mechanical properties of glass-epoxy laminated composite plate

E_1 (GPa)	E_2 (GPa)	G_{12} (GPa)	$\mathcal{V}_{12}$	X_t (MPa)	Y_t (MPa)	X_c (MPa)	Y_c (MPa)	S (MPa)	V_f (%)
31.0	10.5	4.8	0.27	821.0	78.0	377.0	137.0	62.0	38

CHAPTER FOUR

EXPERIMENTAL STUDY

4.1 Introduction

Mechanical tests were performed on a bolted joints in angle-ply of [0/45/30/-30/-30/30/45/0]$_s$ glass-fiber reinforced epoxy for different range of specimen geometry and tightening torque. The strength of bolted joints with various values of tightening torque (T = 0, 3, and 6 Nm), constant width-to-diameter ratio (W/D=6) and the edge distance-to-hole diameter ratio (E/D= 3, 4, 5) in tension and four point bending moment was determined, experimentally.

4.2 Definition of the Problem Statement

4.2.1 Tension

An experimental study, which involved over 54 tests to failure and percentages of failure, was carried out on the effects of geometry and tightening torque in single-lap, single-bolt joints under tension and four point bending moment. The specimen geometry is shown in Figure 4.1. The joint geometry is based on the ASTM standard D 5961/D 5961 M. The geometric ratios, W/D = 6, E/D= 3, 4, 5 and D/t = 1.6, were designed to induce bearing failure in tension tests. The nominal laminate thickness was 3.8 mm when cured. The bolts used were steel fasteners with nominal diameter 6 mm. Steel nuts together with steel washers were also used.
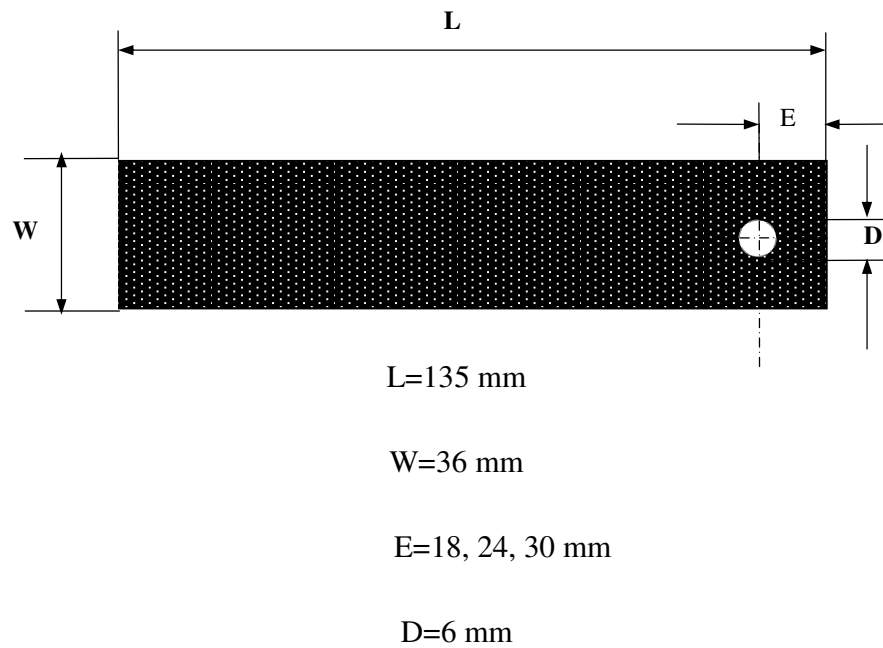
L=135 mm

W=36 mm

E=18, 24, 30 mm

D=6 mm

Figure 4.1 Dimensions of bolted joint specimen

In the tension tests as shown in Figure 4.2 two plates adjoined to each other with fasteners and a uniform tensile load P is applied to the plates. The load is parallel to the plate and is symmetric with respect to the centerline in the tension that it is possible by use tabs that adhered on the end of plates. These tabs also eliminate the secondary bending effects during tension test and obtain symmetric geometry at bending test.
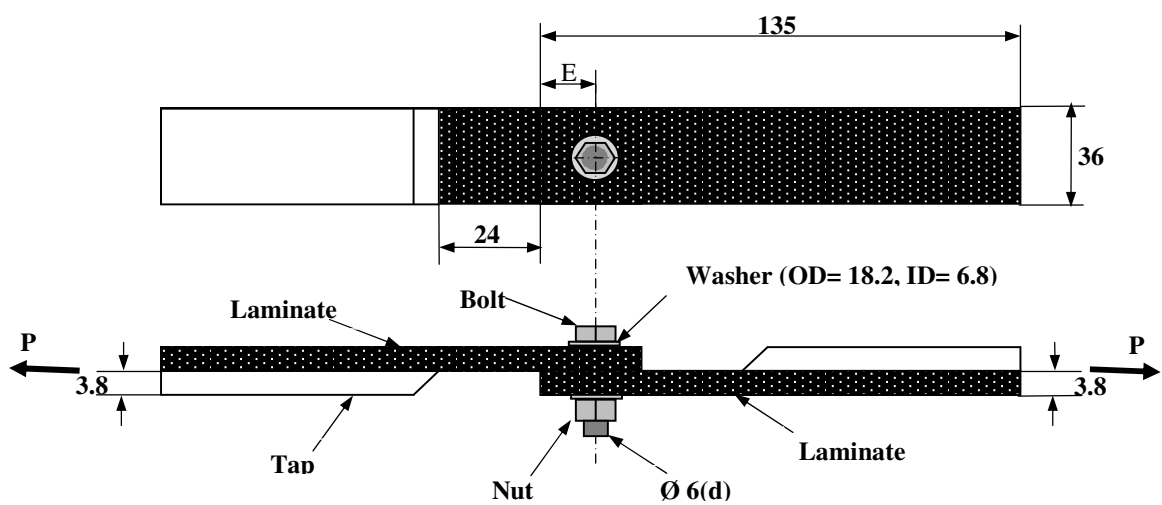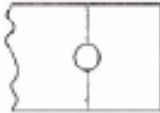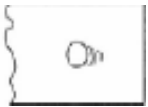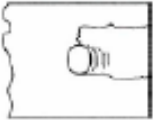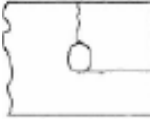

Figure 4.2 Dimension of bolted joint in tensile test

Mechanically- fastened joints under tensile loads generally fail in three basic modes, referred to as net-tension mode, shear out mode, and bearing mode.. In practice combinations of these failure modes are possible. These modes are shown in Table 4.1.

Table 4.1 Typical failure modes for bolted joints

Failure Modes		Comment
Shear out		Caused by stresses and occurs along shear out planes on hole edge, typical failure mode when end distance is short
Tensile (net-tension)		Caused by tangential tensile or compressive stresses at the edge of the hole. For uniaxial loading conditions, failure occurs when bypass/bearing stress ratio is high (or W/D is hinge)
bearing		Occurs in area adjacent to contact area due to compressive stresses, likely when bypass/bearing stress ratio is low (or W/D is low), strongly effected by through-thickness clamping force.
Bearing/shear out		
Bearing/tension/shear out		Mixed-mode
Tension/shear out		

Net tension occurs catastrophically and presents the least strength. Designers are required to obtain the optimum E/D and W/D ratios to get the bearing mode, which shows the highest strength in bolted-joint uses.

4.2.2 Four Point Bending

In the four points bending tests similar to tension test case after adhered the tabs on the plates then plates joined together with fasteners and a uniform pressure load P is applied to the plates as shown in Figure 4.3. The failure mode for the bending moment test is the same mode for all, so that, all of the test specimens fail in transverse direction, similar to net-tension, near the bolt hole. The initial failure starts on the surface layers of the compressive side of the plate.
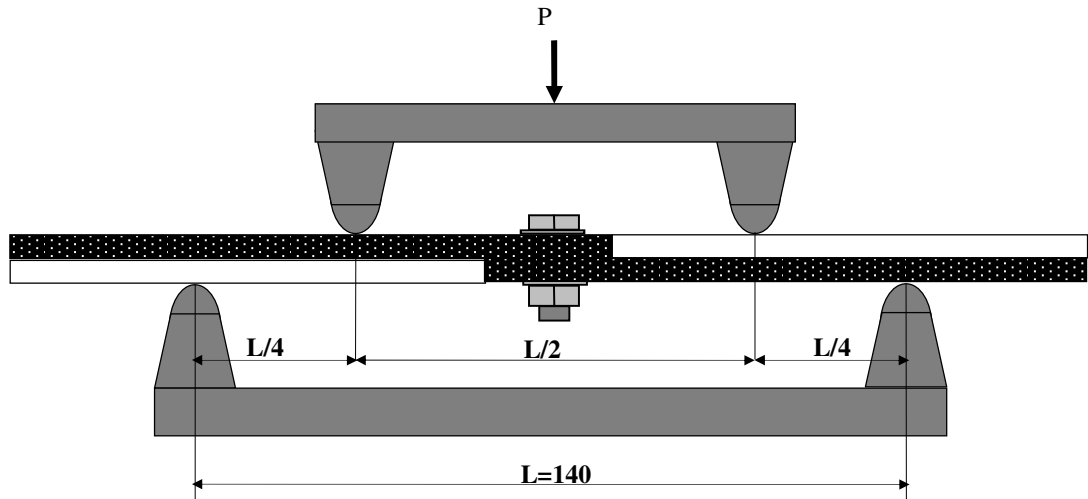
Figure 4.3 Dimension of bolted joint in four point bending test

4.3 Production of the Laminated Composite Plate

The laminated composite plates used in experiments were produced at Izoreel Firm in Izmir. Two different lamina configurations were selected.$[0^o]_8$ laminates for measuring the properties of composite material and $[0/45/30/-30/-30/30/45/0]_s$ to determine the effects of geometry and tightening torque on bolted joint loaded laminated composites. All laminated plates balanced about the mid-plane both prevent thermal distortion for the period of production and to eliminate twisting and bending when under tension. All laminated composite plate were produced E-glass fiber and epoxy resin using press

mould technique. Additionally, for matrix material, epoxy CY225 and hardener HY225 were mixed in the mass ratio of 100:80. The epoxy resin and hardener mix was applied to the fibers. Then, fibers were coated with this mix. Following plies were placed one upon another as required stacking sequence. A hand roller was used to compact plies and take away entrapped air that could later lead to voids or layer separations. During the manufacturing process, the mold and lay-up were covered with a release material. Just the once the matrix material and fibers are combined, it is necessary to apply the proper temperature and pressure for specific periods of time to manufacture the fiber-reinforced laminated composite plate. Therefore, resin agnate fibers were positioned in the mold for curing. These laminas were stuck on each other by hydraulic press. The press generates the pressure and temperature required for curing. Volume fraction of the glass fiber was approximately 38 %. The mould was closed down to give the nominal thickness. The glass fiber/epoxy material was cured at 120^oC under 250 KPa pressure for 2 hours. Then the laminates were cooled to room temperature under press. Finally, laminated composite plate removed from press and cut to specimen dimensions.

In this study glass fiber reinforced epoxy nano-composites also were produced for compare their mechanical properties with glass fiber reinforced epoxy (GFRE) composite. These nano-composites with %2.5, %5 and without nano carbon were produced in the Composite Laboratory at Dokuz Eylul University. The laminated composite specimens were prepared by vacuum assisted resin infusion molding method (Gören & Ataş, 2008). Then the mechanical properties was measured according to described in Chapter Three, the result given in Table 4.2. As seen the mechanical properties of glass fiber reinforced epoxy nano-composites are less than the glass fiber reinforced epoxy (GFRE) composite. Therefore continuing studies in this regard were regardless for now.

Table 4.2 Mechanical properties of glass-epoxy and nano-carbon galas-epoxy laminated composite plates

Composite material	E_1 (GPa)	E_2 (GPa)	ν_{12}	X_t (MPa)	Y_t (Mpa)	X_c (Mpa)	Y_c (Mpa)
GFRE	29.0	12.5	0.26	676.0	144.0	428.0	210.0
GFRE with %2.5 nano carbon	22.0	10.5	0.21	380.0	91.0	277.0	183.0
GFRE with %5 nano carbon	25.0	11.5	0.23	421.0	108.0	290.0	194.0

4.4 Preparation of Specimens

Woven glass–fiber of sixteen layer composite blanks is cut into rectangle shapes for testing through a diamond-impregnated slitting saw. All cut edges were finished using a fine silicon carbide paper to remove any edge defects. The 6 mm holes, typical in size of fasteners used in many structural assemblies, were drilled using a steel drilling tool.

Specimens for each group were produced in the following manner: while keeping the W/D ratio constant as 6, the E/D ratio is varied as 3, 4 and 5. After the specimens are prepared 3 groups then two of plates joined to each other with fasteners and a tightening torques applied to fasteners that values of the tightening torques were (T=0, 3, 6). Therefore total of the tests was done during the study become 54. Thus 27 test done for each case of tension and four points bending, so that three test for each position.

4.5 Testing Process

The tests were conducted with reference to D 5961/D 5961 M at a room temperature of 20°C. In the tension tests when the specimens were placed in the testing machine, taking care to align the longitudinal axis of the specimen. The experiments were performed by means of a custom fixture on the SHIMADZU Testing Machine with a speed of 1mm/min. Figure 4.4.
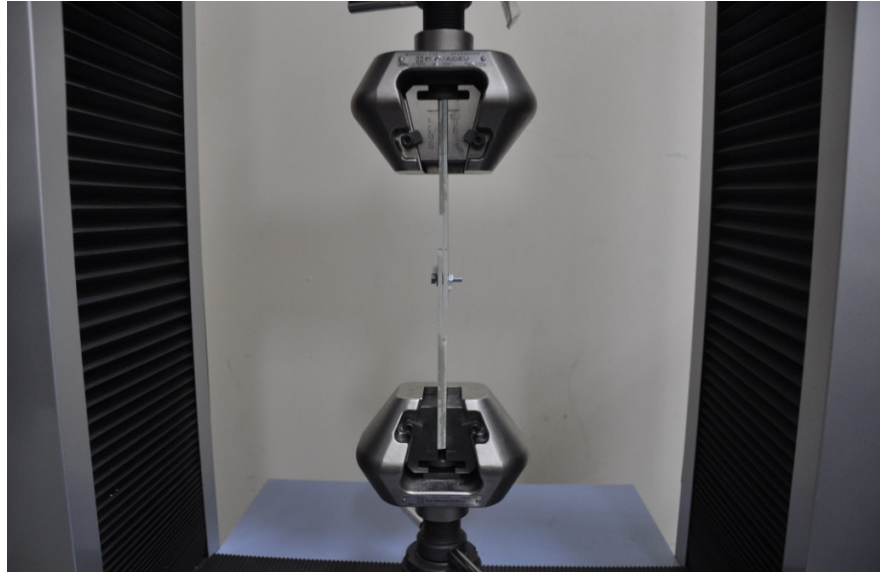
Figure 4.4 bolt loaded glass-epoxy laminated composite test process

For all position, three specimens were tested. Mean values and standard deviations were calculated. Bearing strengths were obtained as follows;

$$\sigma_b = \frac{P_{max}}{Dt} \tag{4.1}$$

Where P_{max} is the failure load, D and denotes the hole diameter and the thickness of the specimen, respectively.

In the four point bending tests when the specimens were placed in the testing machine, was attempted that the length proportion regarding during the tests, as shown in Figure 4.3. The experiments were performed by means of a custom fixture on the SHIMADZU Testing Machine with a speed of 1mm/min. Figure 4.5 show the four point bending process.
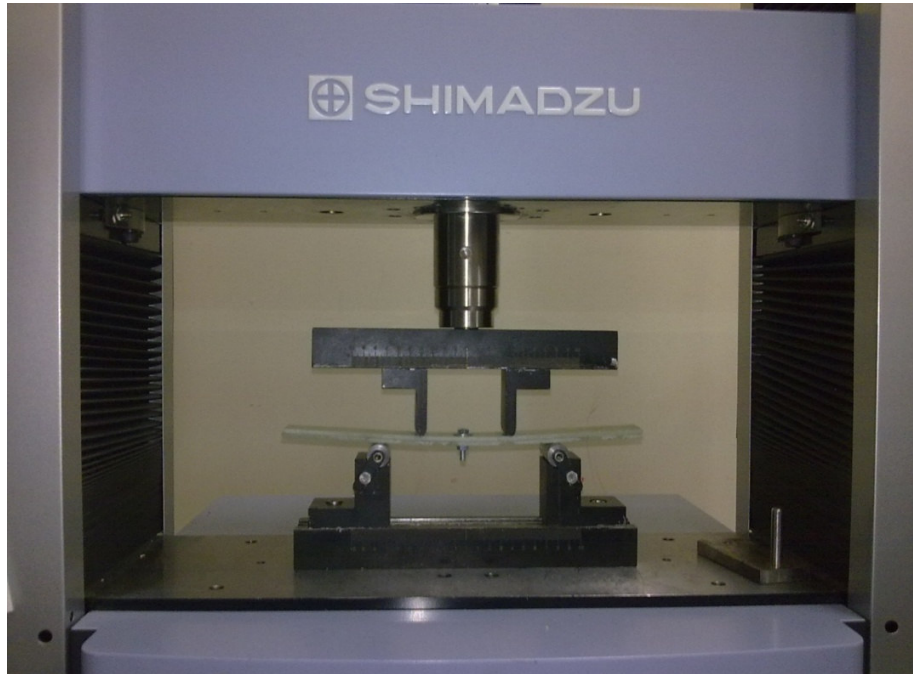
Figure 4.5 Bolt loaded glass-epoxy laminated composite four point bending test process

Bending strength at four point bending tests was calculated as follows;

$$M = \frac{P_{max} \cdot L}{8}$$

$$I = \frac{t^3(W-D)}{12} \tag{4.2}$$

$$\sigma = \frac{M \cdot \frac{t}{2}}{I} = \frac{3P_{max}L}{4t^2(W-D)}$$

Where P_{max} is the failure bending load, L, W, D and t denotes the length, width, hole diameter and the thickness of the specimen, respectively.

CHAPTER FIVE

RESULT AND DISCUSSION

5.1 Introduction

In this chapter, a detailed discussion is given the light of experimental study results of single-lap bolted glass-epoxy laminated composite joints.

5.2 Failure Modes

Three different failure types were observed during the studies that published previously: bearing, net tension and shear-out. The typical load/displacement curves for the bearing, net tension and shear-out failure types are illustrated in figure 5.1.
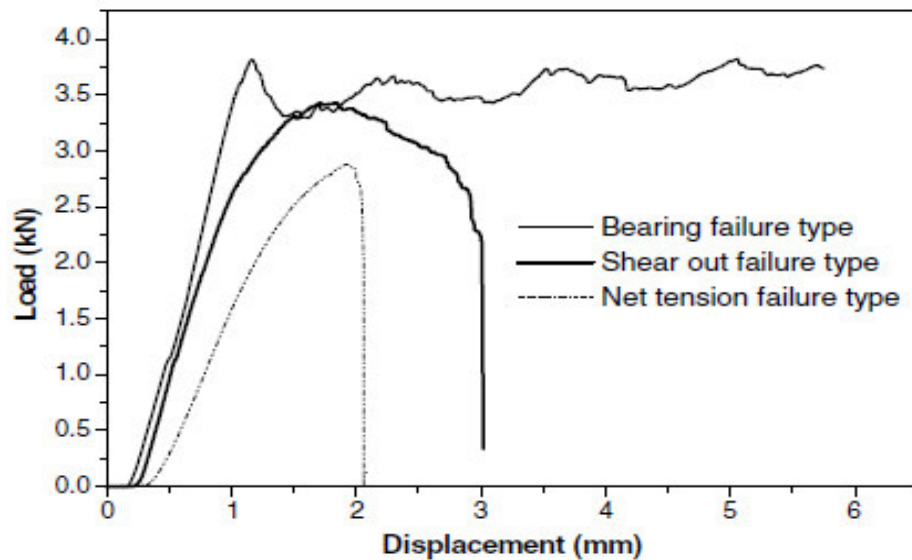
Figure 5.1 Load/displacement curves of different failure types: (a) bearing failure type, (b) shear-out failure type and (c) tension failure type.

As seen in Figure 5.1; as the pin displacement is increased, the load increased in an almost linear manner. Then, failure started at different loads for different geometries and ply orientations and the load reached a peak (first peak). After reaching maximum load there is not a rapid drop in force values in bearing type failure during pin loading. Load displacement curves show valleys, peaks and plateaus highly depending on types of ply orientations and geometry. The matrix fracture, delaminations between laminates, fiber

breakages, fiber matrix interface deformations, fiber buckling, etc. are the main reasons for the zigzag formation of the curve. This gives adequate energy absorption during deformations because it goes on bearing the applied load till the end of the complete failure of the material which improves the safety of the joint. This type of connection has damage tolerance before the fracture of the material.

On the other hand, in tension type failure, propagation direction of the crack is perpendicular to the direction of the applied load. Load values rapidly drop to zero in a short time after reaching its maximum. There is no dramatical load drop during test in shear-out type loading compared to tension type failure the joint is comparatively deformed under higher load and absorbing higher energy compared to the tension type failure. However, both tension and shear-out type failures are not as safe as bearing type failure.

In this study each test specimen was loaded until the occurrence of the last failure. The general behavior of the composite joint was determined from the load–displacement curves. Two different failure types were observed during the tensile tests of the study: Bearing, net tension and the combination of these modes. The typical load/displacement curves are shown in Figure 5.2 (a, b). For T=3 and E/D=3, and the complete failure modes can be seen in Table 5.1.
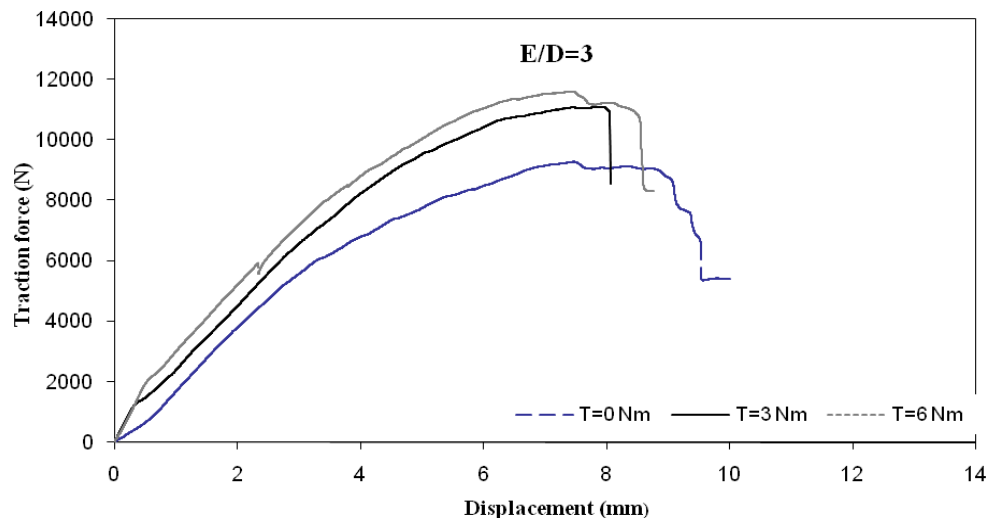
(a)
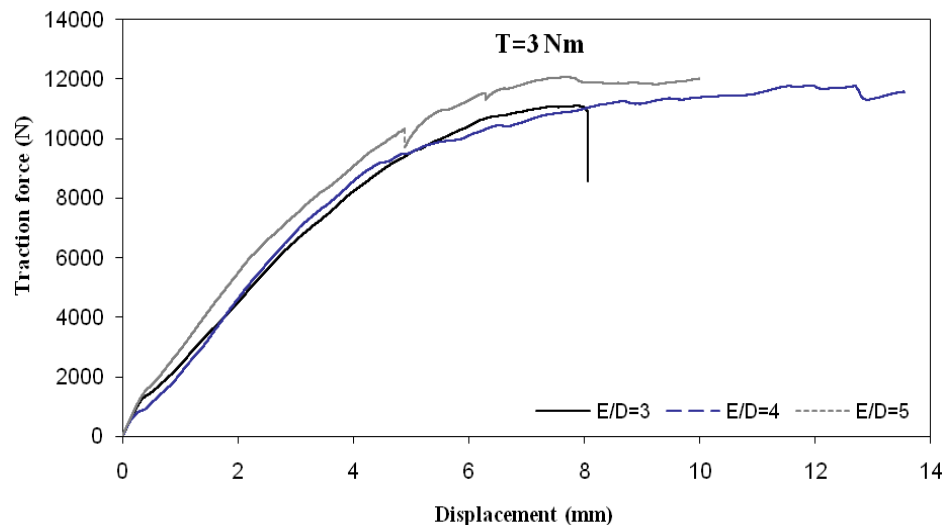
(b)

Figure 5.2 Force-displacement curves; **a)** E/D=3 and tightening torque variable, **b)** T=3 Nm and E/D variable

Table 5.1 Failure modes and values of the failure load and bearing strength

N: Net-tension mode, **B:** Bearing mode

	T (Nm)	E/D	specimens	Failure load and failure modes		
				Failure mode	Failure load (N)	Bearing strength (MPa)
W/D=3	0	3	1	N	9509	220.11
			2	N	9203	213.03
			3	N	10526	243.65
			average		**9746**	**225.60**
		4	1	N	9878	228.65
			2	N	11311	261.82
			3	N	10622	245.87
			average		**10966**	**253.80**
		5	1	N	11149	258.07
			2	N+B	11776	272.59
			3	N+B	12605	291.78
			average		**11843**	**274.10**
	3	3	1	N	10648	246.48
			2	N	10832	250.74
			3	N	10260	273.50
			average		**10579**	**244.90**
		4	1	N	12272	284.07
			2	N+B	12533	290.11
			3	N+B	12215	282.75
			average		**12340**	**285.60**
		5	1	B	11857	274.46
			2	B	12351	285.90
			3	B	12703	294.05
			average		**12303**	**284.80**
	6	3	1	N	11318	261.99
			2	N	11119	257.38
			3	N	11408	264.07
			average		**11215**	**259.60**
		4	1	N+B	12410	287.26
			2	N+B	12505	289.46
			3	N+B	12615	292.01
			average		**12510**	**289.60**
		5	1	B	12627	292.29
			2	B	12349	285.85
			3	B	12124	280.64
			average		**12360**	**286.20**

The photographs of some tested specimens with various failure modes are illustrated in Figure 5.3 as examples of observed failure modes. The net tension failure mode is not occurred lonely because net tension mode occurs when the W/D ratios are very small but in this study W/D=3 and it's not very small. The bearing failure modes are observed for some specimens that are having big E/D ratio and tightening torque.
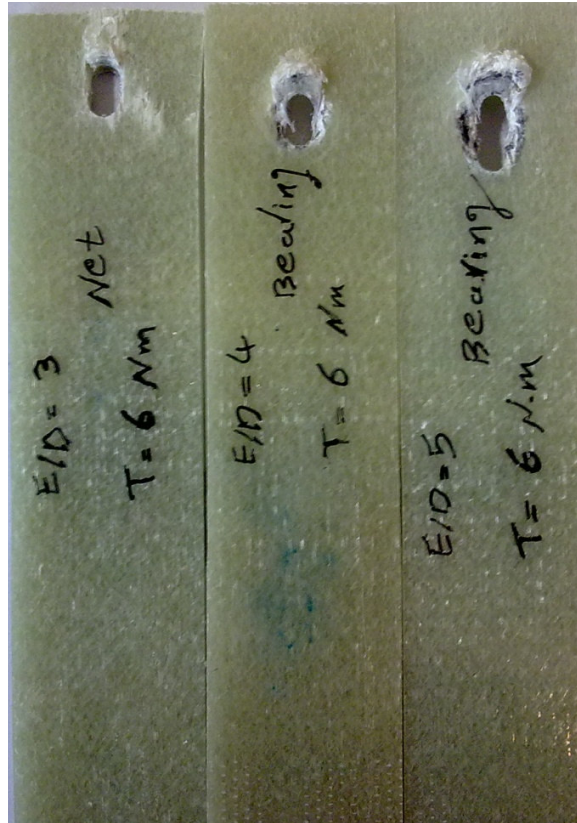

Figure 5.3 The photograph of some tested specimens at traction
for T=6 Nm and variable E/D ratio with various failure modes.

The failure mode for the bending moment test is the same mode for all, so that, all of the test specimens fail in transverse direction, similar to net-tension, near the bolt hole. The initial failure starts on the surface layers of the compressive side of the specimen. The typical failure bending moment curves are shown in Figure 5.4 (a, b) for T=3 and E/D=3, and the complete failure load values and bending strength can be seen in Table 5.2. It seems that the failure modes are similar to the net-tension mode. The curves fall down suddenly after failure occurring. The photograph of this mode is shown in Figure 5.5.
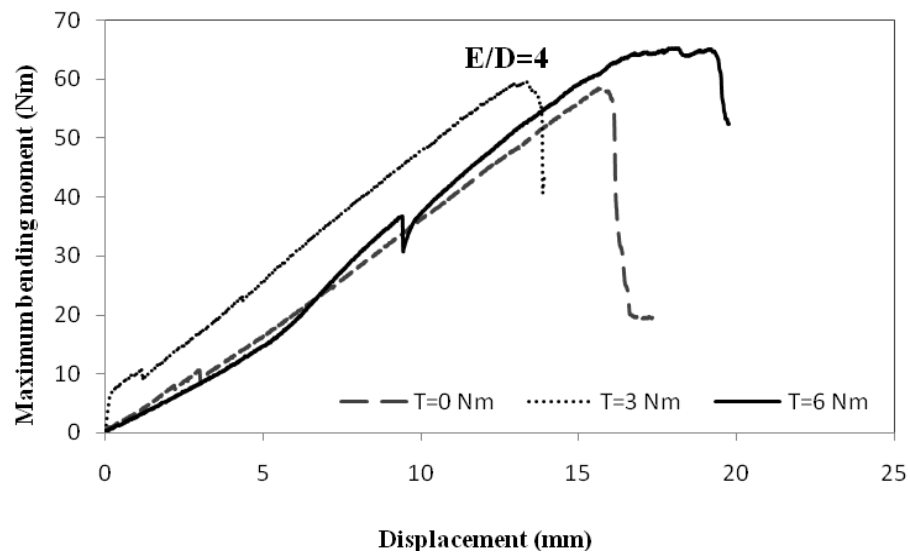
(a)
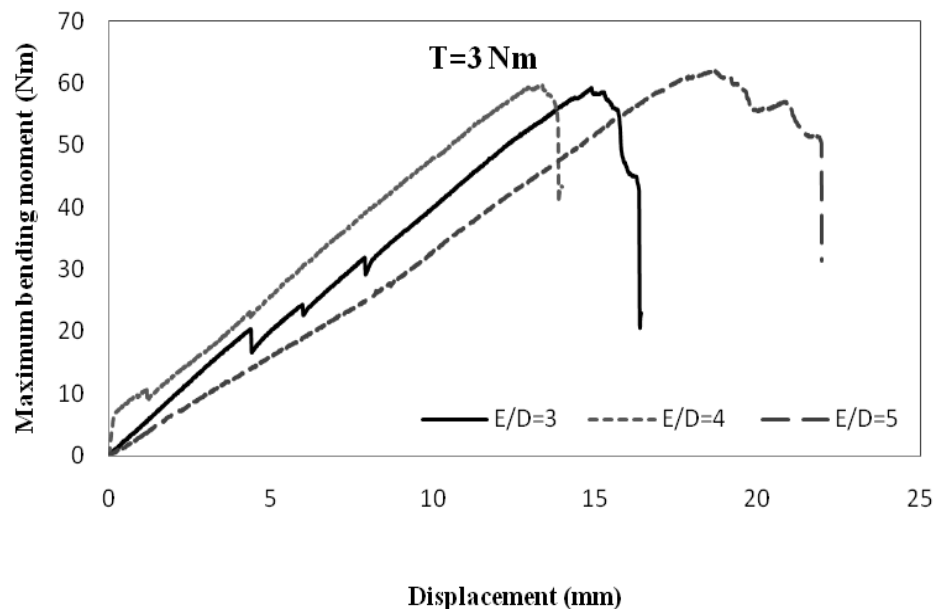
(b)

Figure 5.4 The moment and displacement curves; a) E/D=4 and tightening torque variable, b) T=3 Nm and E/D variable

Table.5.2 Failure loads values and bending strength

| | T (Nm) | E/D | specimens | Failure load and bending strength | | |
				Failure load (N)	bending strength (MPa)	Failure mode
W/D=3	0	3	1	2930	710.18	Similar to net-tension
			2	2291	555.29	
			3	2642	640.37	
			average	**2621**	**635.28**	
		4	1	3335	808.34	
			2	2030	492.03	
			3	2291	555.29	
			average	**2552**	**618.55**	
		5	1	3296	798.89	
			2	3669	889.30	
			3	3436	832.82	
			average	**3467**	**840.33**	
	3	3	1	3383	819.97	
			2	3315	803.49	
			3	3225	781.68	
			average	**3307**	**801.55**	
		4	1	2609	632.37	
			2	3786	917.65	
			3	3394	822.64	
			average	**3263**	**790.89**	
		5	1	3531	855.85	
			2	3590	870.15	
			3	3490	845.91	
			average	**3531**	**855.85**	
	6	3	1	3031	734.66	
			2	3404	825.06	
			3	3141	761.32	
			average	**3192**	**773.68**	
		4	1	3727	903.35	
			2	3590	870.15	
			3	3412	827.00	
			average	**3576**	**866.75**	
		5	1	3462	839.12	
			2	3394	822.64	
			3	3174	769.32	
			average	**3343**	**810.28**	
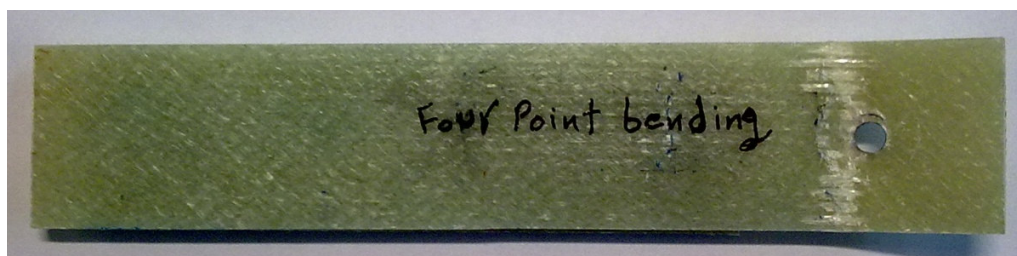
Figure 5.5 The failure mode's photograph of tested specimen at four point bending moment

5.3 Effects of E/D Ratio and Tightening Torques

In this section, 0, 3 and 6 Nm tightening torques were applied to the test specimens before loading and the effects of these torques were examined. Thus, the effects of the increasing tightening torque on failure behavior and bearing strength at tension and bending strengtht under four point bending tests were investigated. The bearing strength was calculated as Equation (4.1)

Figure 5.6 shows the influence of tightening torque on the behavior of bearing failure of bolted joint specimens with constant W/D = 3 and variable E/D=3-5 in the tensile test. The results in this figure indicate that, the bearing strength of the bolted joint increases by increasing the tightening torque. Therefore, the tensile loads under 6 Nm tightening torques are higher than those under 0 and 3 Nm tightening torques, in general. In addition, the axial failure loads under 3 and 6 Nm tightening torques are usually calculated very close to each other. Nevertheless, the failure loads without tightening torque are small in comparison with the other tightening torques. Therefore, it seems that increased values of tightening torques satisfy a strong structure so that the load carrying capacity of the single-lap bolted joint of the fiber reinforced composite plates increases by increasing the tightening torque. But it seems that failure bearing strength decreases or does not change with continuous increase of tightening torque.
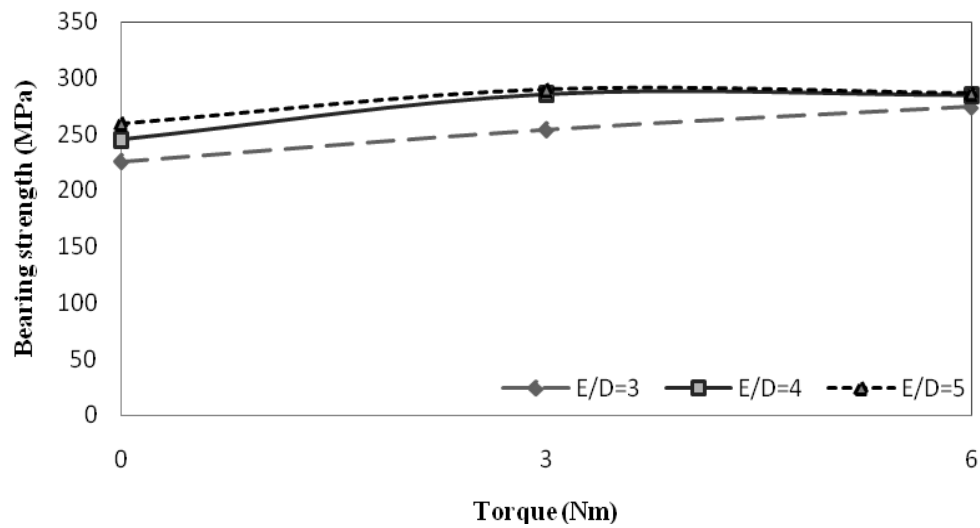
Figure 5.6 The effect of E/D and torque on the bearing strength in traction test

Traction or axial forces versus displacement under T=0, 3, 6 Nm for E/D=3 are shown in Figure 5.2 (a). As seen, when the tightening torque increases, the failure load reaches higher values. It is also seen that the net-tension failure mode occurs for E/D=3. Traction forces versus displacement under T=3 Nm for E/D=3-5 are shown in Figure 5.2 (b). It seems that net-tension failure mode occurs for E/D=3, nevertheless, the bearing failure mode occurs for E/D=4, 5. When E/D increases, the failure mode becomes the bearing mode. The bearing mode is preferred to other modes.

The effect of the E/D ratio on the bearing strength under T=0, 3, 6 Nm tightening torques is shown in Figure 5.7. As seen, when E/D ratio increases the bearing strength increases gradually. The bearing strength represents a close result under T=3 and 6 Nm tightening torques.
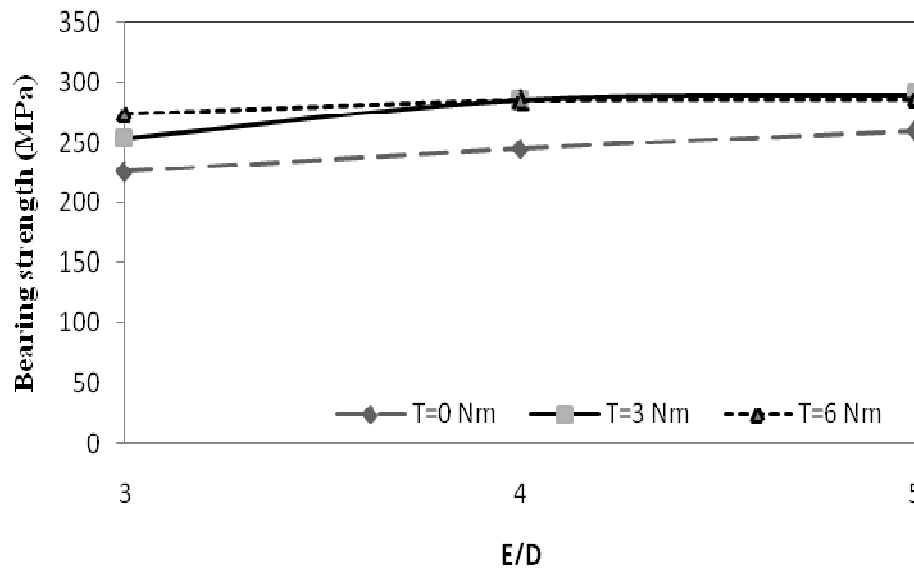
Figure 5.7 The effects of E/D ratio on the bearing strength

The effect of the tightening torques on the bending strength was investigated by conducting the four point bending moment test. A typical curve is shown in Figure 5.8. It is seen that when the torque increases, the bending strength increases for E/D=3, 4, 5. The ratio of E/D=5 satisfies the highest bending strength. The 3 and 6 Nm torques produce close results for E/D=3, 4, 5.
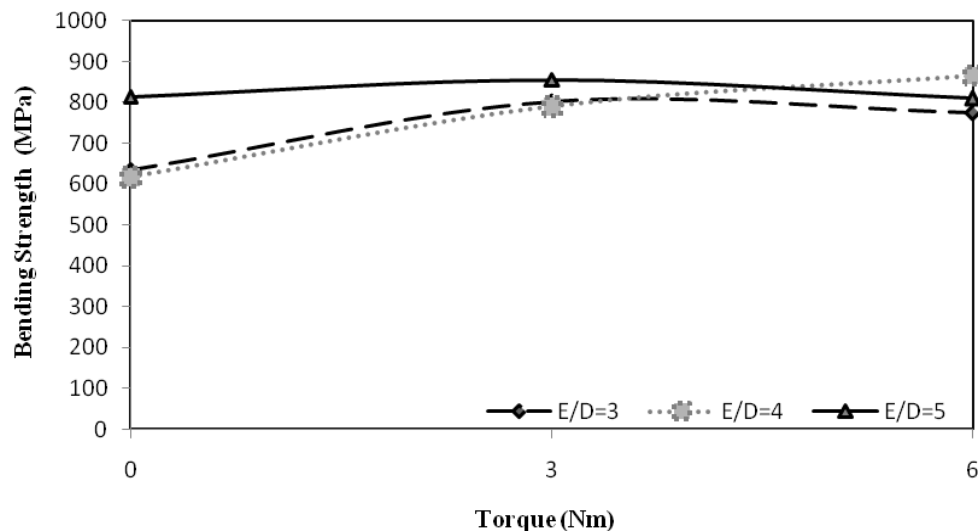

Figure 5.8 The effect of tightening torque on the bending strength

The influence of E/D ratio on the bending strength for T=0, 3, 6 Nm is shown in Figure 5.9. It seems that T=3 and 6 Nm tightening torques produce close values for E/D=3-5. Moreover, the bending strength is small when the tightening torque equals to zero, in comparison with the values for T=3 and 6 Nm.
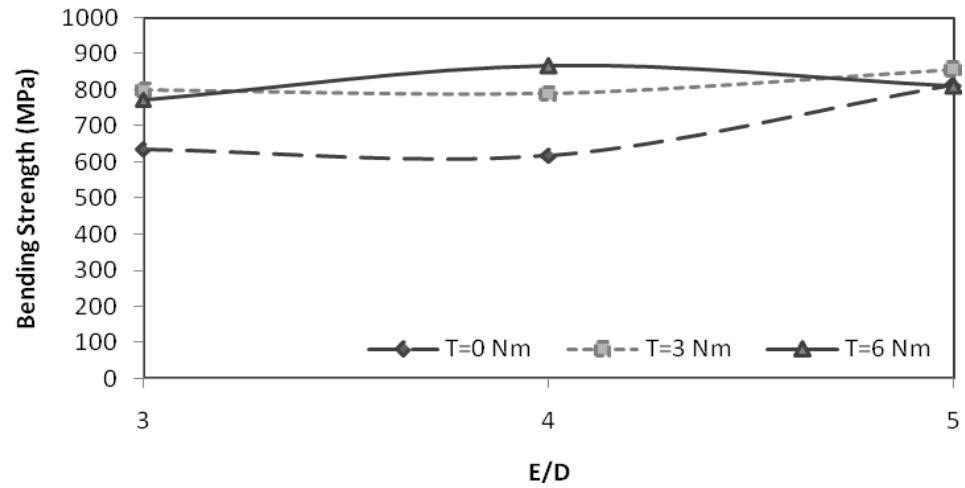

Figure 5.9 The effect of E/D on the bending strength

CHAPTER SIX
CONCLUSIONS

The failure of the single-lap joints in glass fiber reinforced epoxy (GFRE) composites with a constant W/D ratio (3) and variable the E/D ratios (3, 4, 5) and tightening torque values (0, 3 and 6 Nm) was examined under axial forces and bending moments. The bending moments were produced by four point bending method. The following results can be concluded from tests:

a)   Under axial traction force, the bearing strength increases when E/D ratio and tightening torque values increases.

b)   The tabs that bonded to the ends of the specimen eliminate the effects of secondary bending.

c)   When the tightening torque increases the maximum bending strength increases

d)   The failure load increases considerably for T=0, whereas it increases slightly and gives close results under T=3, 6 Nm bending moments. It is almost linear for E/D=5. As a result of this, the 3 Nm tightening torque will be generally adequate for this joint.

e)   The bending strength increases when E/D increases without a tightening torque or T=0.

f)   In the bending tests, the failure firstly begins on the compressive side and the joint fails at the center near the bolt, because of the excessive delaminations on the compressive side, due to the small strength of X_c.

REFERENCES

Abd-El-Naby, S. F. M., Hollaway, L. (1993) The experimantal behaviour of bolted joints in pultruded glass/polyester material. Part 1: singlebolt joints. *J Comp Mater*, *24*,531–8.

Aktas, A., & Dirikolu M. H. (2003). The effect of stacking sequence of carbon epoxy composite laminates on pinned-joint strength. *Compos Structures*, *62*,107–11.

Aktas, A., & Kurakuzu, R. (1999). Failure analysis of two dimensional carbon–epoxy composite plate pinned joint. *Mech Compos Mater Struct*, 347–61.

Apalak, M. K., Apalak, Z. G., Gunes R., Karakas, E. S. (2003). Steady-state thermal and geometrical non-linear stress analysis of an adhesively bonded tee joint with double support. *International Journal of Adhesion and Adhesives, 23,* 115-130.

ASTM standard D 5961/D 5961M-96. (2003). *Standard test method for bearing response of polymer matrix composite laminates.*

Camanho, PP., Bowron, S., & Matthews, FL. (1998) Failure mechanisms in bolted CFRP. *J Reinf Plast Comp*, *17*,205–33.

Chang FK., Scott RA., & Springer GS. (1982). Strength of mechanically fastened composite joints. *J Compos Mater*, 470–94.

Chen, JC., Chiu, CH., & Chin H. (1994) On the influence of weave structure on pinloaded strength of orthogonal 3D composites. *J Comp Mater*, *30*,251–62

Collings TA. (1982). On the bearing strengths of CFRP laminates. *Composites*, 241–52.

Collings, TA. (1977). The strength of bolted joints in multi-directional CFRP laminates. *Composites* , 43–55.

Crews, JHJ. (1981). *Bolt-bearing fatigue of a graphite/epoxy laminate.* In: Kedward KT, editor. Joining of composite materials, ASTM STP 749. American Society for Testing and Materials*, p*.131–44.

Daniel, I. M., & Ishai, O. (1994). *Engineering Mechanics of Composite Materials*. Oxford University Press. New York Oxford.

DiNicola AJ., & Fantle SL. (1993). Bearing strength behaviour of clearance fit fastener holes in toughened graphite/epoxy laminates. In:Camponeshi Jr ET, editor. *Composite materials: testing and design*. ASTM STP 1206. Philadelphia: American Society forTesting and Materials, p. 220–37.

DODSSP, *Polymer Matrix Composites*, MIL-HDBK-17, DODSSP, Naval Publications and Forms Center, Standardization Documents Order Desk, Building 4 D, 700 Robbins Ave., Philadelphia, PA 19111-5094.

Eriksson, I. (1990). On the bearing strength of bolted graphite/epoxy laminates. *J Compos Mater*, *24*,1264–9.

Fan, WX., & Qiu, CT. (1993). Load distribution of multi-fastener laminated composite joints. *Int J Solids Struct*, *30(21)*, 3013–23.

Gibson, R.F. (1994). *Principals of Composite Material Mechanics.* McGraw-Hill.

Goren, A., & Atas, C. (2008). Manufacturing of polymer matrix composites using vacuum assisted resin infusion molding, *Archives of Materials Science and Engineering 34* 117-120.

Hamada, H., & Maekawa, ZI. (1996). Strength prediction of mechanically fastened quasi-isotropic carbon/epoxy joints. *J Compos Mater*, *30*, 1596–612.

Ireman, T. (1998). Three-dimensional stress analysis of bolted single-lap composite joints. *Composite structures*, *43*, 195-216.

Shyprykevich, P. (1995) Characterization of bolted joint behaviour: MIL-HDBK-17 Accomplishments at standardization. *J Composites Technology and Research, JCTRER*, *17(3)*, 260–70.

Jones, R. M. (1999). *Mechanics of Composite Materials* (2nd ed.). US: Taylor & Francis Inc

Khashaba, UA. (1996). Notched and pin bearing strengths of GFRP composite laminates. *J Compos Mater*, 2042–54.

Kim, RY. (1987). *Fatigue strength. ASM Engineered Materials Handbook, vol.1*. ASM International Handbook Committee, p.436–44.

Mallick, P. K. (1993). *Fiber-reinforced composites materials, manufacturing, and design.* (2 nd ed). New York: Marcel Decker.

Matthews F.L., Davies., G.A.O., Hitchings, D., Soutis, C. (2000). *Finite element modelling of composite materials and structures*, Cambridge: Woodhead Publishing Ltd. and CRC Press LLC.

Mazumdar, S.K., (2002) *Composites manufacturing : materials, product, and process Engineering*, USA: CRC Press LLC

McCarthy, MA., Lawlor, VP., Stanley, WF., McCarthy, CT. (2002). Bolt– hole clearance effects and strength criteria in single-bolt, single lap, composite bolted joints. *Compos Sci Technol*, *62*, 1415–31.

McCarthy, MA., & McCarthy, CT. (2003). Finite element analysis of the effects of clearance on single-shear, composite bolted joints. *J Plast Rubber Compos*, *32(2)*, 65–70.

Meola, C., Squillace, A., Giorleo, G., Nele, L. (2003). Experimental characterization of an innovative glare fiber reinforced metal laminate in pin bearing. *J Compos Mater*, *37*, 1543–52.

Naik, RA., Crews, Jr. JH. (1986). Stress analysis method for a clearance-fit bolt under bearing loads. *AIAA Journal*, *24(8)*, 1348–53.

Okutan, B., Aslan, Z., & Karakuzu, R. (2001). A study of effects of various geometric parameters on the failure strength of pin-loaded wovenglass–fiber reinforced epoxy laminate. *J Compos Sci Technol*, 1491–7.

Okutan, B. & Karakuzu, R. (2002). The failure strength for pin-loaded multidirectional fiber-glass reinforced epoxy laminate. *Journal of Composite Materials, 36,* 2695–2712.

Pierron, F., Cerisier, F., & Lermes, MGA. (2000). Numerical and experimental study of woven composite pin-joints. *J Compos Mater, 34*, 1028–53.

Richardson, T. (1987). *Composites : A Design Guide*. Industrial Press Inc., New York

Shyprykevich, P. (1995). Characterization of bolted joint behaviour: MILHDBK- 17 Accomplishments at standardization. *Journal of Composites Technology and Research*, *17(3),* 260–70.

Staab, G. H. (1992). *Laminar Composites*. Butterworth Heınemann

Tong, L. (2000). Bearing failure of composite bolted joints with non-uniform bolt-to-washer clearance. Compos Part A: *Appl Sci Manufact*, *31*, 609–15.

Wang, HS., Hung, CL., & Chang, FK. (1996). Bearing failure of bolted composite joints. Part I: experiments. *J Compos Mater*, *30(12)*, 1284–313.

Whitworth, HA., Othieno, M., & Barton, O. (2003). Failure analysis of composite pin loaded joints. *Compos Struct, 59*, 261–6.

Wu, PS., & Sun. CT. (1998). Bearing failure in pin contact of composite laminates. *AIAA J*, *36(11)*, 2124–9.